

This is an Open Access document downloaded from ORCA, Cardiff University's institutional repository:<https://orca.cardiff.ac.uk/id/eprint/107992/>

This is the author's version of a work that was submitted to / accepted for publication.

Citation for final published version:

Huthmann, Florian, Yudovskaya, Marina, Kinnaird, Judith, McCreesh, Matthew and McDonald, Iain 2018. Geochemistry and PGE of the lower mineralized zone of the Waterberg Project, South Africa. *Ore Geology Reviews* 92 , pp. 161-185. 10.1016/j.oregeorev.2017.10.023

Publishers page: <https://doi.org/10.1016/j.oregeorev.2017.10.023>

Please note:

Changes made as a result of publishing processes such as copy-editing, formatting and page numbers may not be reflected in this version. For the definitive version of this publication, please refer to the published source. You are advised to consult the publisher's version if you wish to cite this paper.

This version is being made available in accordance with publisher policies. See <http://orca.cf.ac.uk/policies.html> for usage policies. Copyright and moral rights for publications made available in ORCA are retained by the copyright holders.



1 Petrogenesis and PGE of the lower mineralized zone of the
2 Waterberg Project, South Africa

3

4 August 28, 2017

5 Huthmann, Yudovskaya, Kinnaird, McCreesh, McDonald

6 **Abstract**

7 The Waterberg deposit is located north of the Northern Lobe of the Bushveld Complex in South
8 Africa and represents a large, **high-grade**, new PGE discovery with the potential to change the
9 local and global **miningPGE** market. The first comprehensive study of the lower ultramafic section
10 of ~~this~~**the exciting** area has been ~~conducted~~**completed**, and ~~below core logging~~; whole-rock chemical
11 analyses and ~~six-element~~ PGE data are presented.

12 The ~~Waterberg Succession in the s~~section studied comprises mineralized harzburgites and marginal
13 ~~orthopyroxenite, rocks~~ overlain by troctolite grading into gabbroic rocks. Whole-rock analyses
14 show geochemical ~~signatures~~**variations** typical of **differentiated assemblages** of cumulus olivine,
15 plagioclase, and pyroxene ~~assemblages~~. Normalized trace element data display HREE depletion,
16 strong positive Eu and Sr anomalies and LREE enrichment. The ~~position of positive as well as~~
17 ~~negative~~**negative** anomalies for Th, Rb, Nb and Ta ~~is~~ are typical for rocks of the Bushveld Complex.
18 Normalized PGE distributions are ~~strongly~~ fractionated (Pd/Ir 177) ~~and~~, Pd-enriched, and Au-
19 ~~poor~~.

20 Emplacement of the ~~rocksmagmas was initiated~~**is** believed to have commenced ~~by~~**with** west-east
21 trending, finger-like intrusions, followed by lateral dilation and emplacement of sulfide droplet-
22 bearing, ultramafic ~~chonolithsmagmas~~. This ~~in turn~~ was followed by a second phase of intrusi**veons**,
23 characterized by sheet-like ~~emplacement~~**bodies** of troctolites. Fractionation of these magmas led to
24 ~~the development of gabbroic rocks that make up the top of the succession. The Waterberg Project~~
25 ~~is located in the Southern Marginal Zone of the Limpopo Belt. This position in a structurally~~
26 ~~active area may have facilitated the creation of space for initial magmas.~~

27 It is argued, that the ~~Waterberg succession~~**mafic to ultramafic succession of the Waterberg Project**
28 ~~does not represent a simple marginal extension of the Aurora Project of the Northern Lobe, nor~~
29 ~~does it directly correlate with the Platreef. It shares geological features, but represents a separate~~
30 ~~magmatic basin.~~

31 The conclusion that the ~~WB~~**Waterberg Succession** does not represent a simple strike extension of
32 the Northern Lobe is excellent news for explorers of the Bushveld Complex. ~~and~~**It** demonstrates,
33 ~~that cooperation of industry and academia, aided by 21st century geophysical techniques, that~~
34 ~~mineralized successions with their own metal budgets~~ can lead to significant discoveries in well-
35 explored terrains.

1 Introduction

The Northern Lobe of the Bushveld Complex hosts the Platreef and includes the world-class ore bodies. The stratigraphy and mineralization of the Northern Lobe has been the topic of many studies in recent years. In the light of the discovery of Main Zone-hosted mineralization in the far north and south of the lobe (Harmer et al., 2004; Maier and Barnes, 2010), the Main Zone of the Bushveld Complex is now the center of renewed attention. The Waterberg Project is located north of the Northern Lobe and represents a large, recent PGE discovery (Huthmann et al., 2016; Kinnaird et al., 2017). The Waterberg Succession is presented, which in a recent publication McDonald et al. (2017) has been interpreted to be (at least in parts) the lateral equivalent of aforementioned Main Zone-hosted PGE occurrences.

The significant Waterberg Pd/Pt mineral system is a >3.5 by 24 km, mafic to ultramafic, lobate intrusion hosting an indicated resource of 24.9 million ounces 4E (Pt+Pd+Rh+Au; 2.5 g/t cut-off) in an upper (T Zone) and lower (F Zone) mineralized zones. Its U/Pb ages of 2059 ± 3 and 2053 ± 5 Ma (Huthmann et al., 2016) overlap within error with the 2.06 Ga age (Scoates and Friedman, 2008; Scoates and Wall, 2015; Zeh et al., 2015) of the Bushveld Complex. Kinnaird et al. (2017) provide an extensive overview of the local geology, the relationship of the succession with its roof rocks, and details of the T and F mineralized zones. In this contribution, the stratigraphy of a small area, hosting the Super F mineralized zone is described in detail. The geology of the overlying units is described in less detail and the reader is referred to the aforementioned upcoming publication.

Drill intercept data from >100 drill holes indicate the presence of discontinuous and variable lithologies in the study area. In this study, a range of drill holes has been logged in detail and below whole-rock major and trace element geochemistry as well as six element PGE data have been compared to available company assays. The data gathered for this study is used to present the first conceptual model for the evolution of the Waterberg Succession. It is argued, that if all aspects are considered, the succession does not correlate directly with units described in the southern half of the Northern Lobe of the Bushveld Complex. Possible correlations with the geology at the Aurora Project (Harmer et al., 2004) immediately to the south are explored in detail in the discussion section.

2 Geology

The 2.06 Ga (Scoates and Friedman, 2008; Scoates and Wall, 2015; Zeh et al., 2015) Bushveld Complex is the largest layered intrusion on Earth and the world's largest repository of magmatic PGE, Cr and V ore deposits (Lee, 1996). It was traditionally believed to consist of 5 lobes with an estimated areal extent of approximately 65 000 km² (Willemse, 1969); however, the intersected ultramafic-mafic rocks at the northern end of the Northern Lobe and recent geophysical studies, however, increase this total areal extent to >90 000 km² (Finn et al., 2015). While Although the lobes were historically interpreted to be separate bodies, more recent re-interpretation of the gravity data allows for the possibility that the Eastern and Western Lobes may be connected at depth (Webb et al., 2004; Finn et al., 2015). Links between the Northern Lobe and the Eastern and Western Lobes are contentious (Cawthorn and Webb, 2001), and links between the

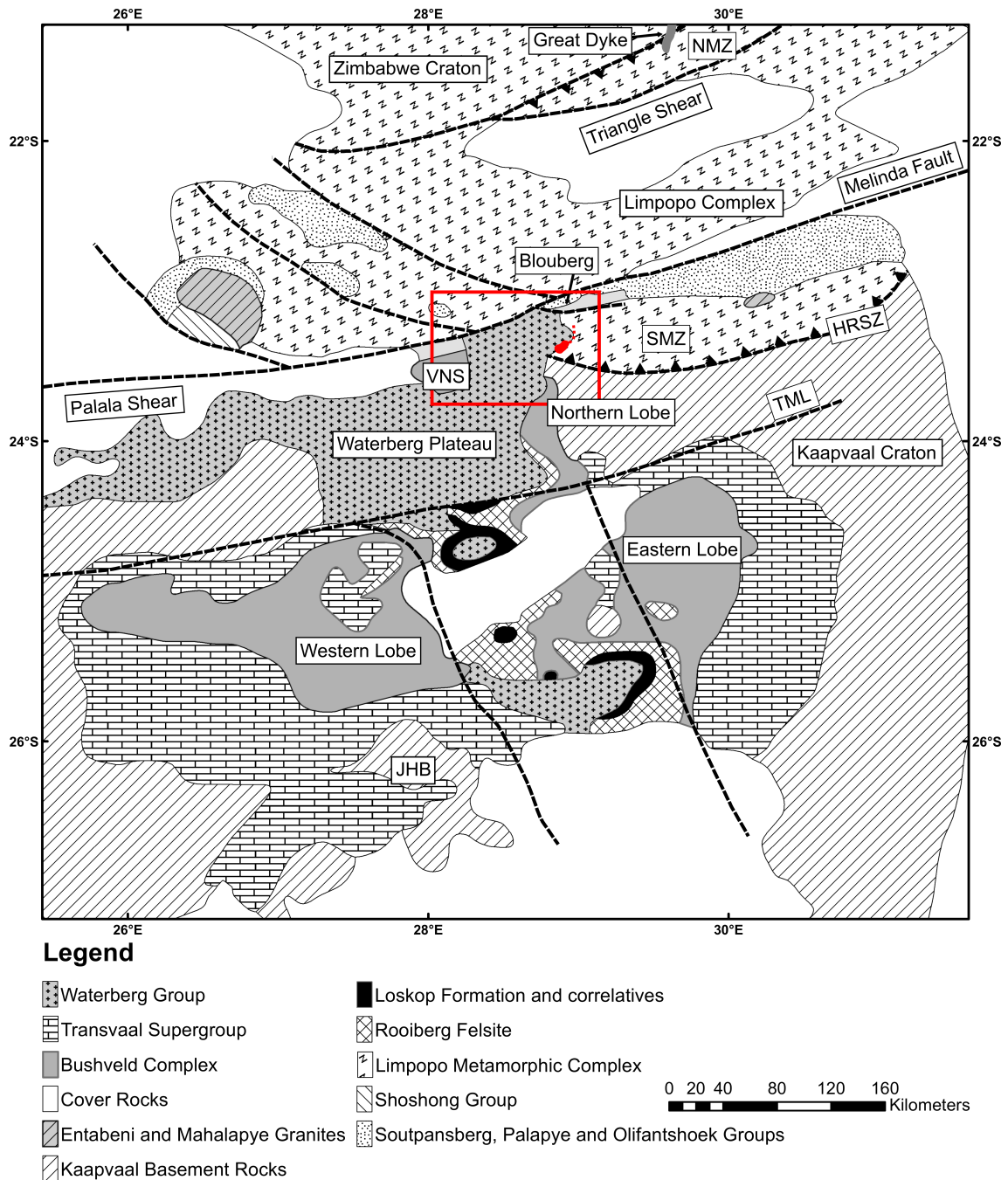


Figure 1: Map showing the distribution of major lithological units in northern South Africa. JHB Johannesburg; SMZ Southern Marginal Zone; NMZ Northern Marginal Zone; TML Thabazimbi-Murchison lineament; HRSZ Hout River Shear Zone. The small rectangle indicates the Waterberg area. Modified after Dorland et al., 2006.

78 Northern Lobe and mineralized rocks at its northern end the Waterberg Project remain to be es-
 79 tablished and will be discussed in this contribution. The controversy also includes the gently
 80 south-dipping Villa Nora Segment (Fig. 1) and its relationship to both the Northern Lobe and the
 81 mafic succession Waterberg Project.

82 The Bushveld Complex comprises heterogeneous, predominantly felsic volcanics, a mafic to ultra-
 83 mafic suite of 7-8 km thickness, plus a granite as well as a granophyre suite (von Gruenewaldt
 84 et al., 1985). The mafic package, also known as the Rustenburg Layered Suite, is subdivided into

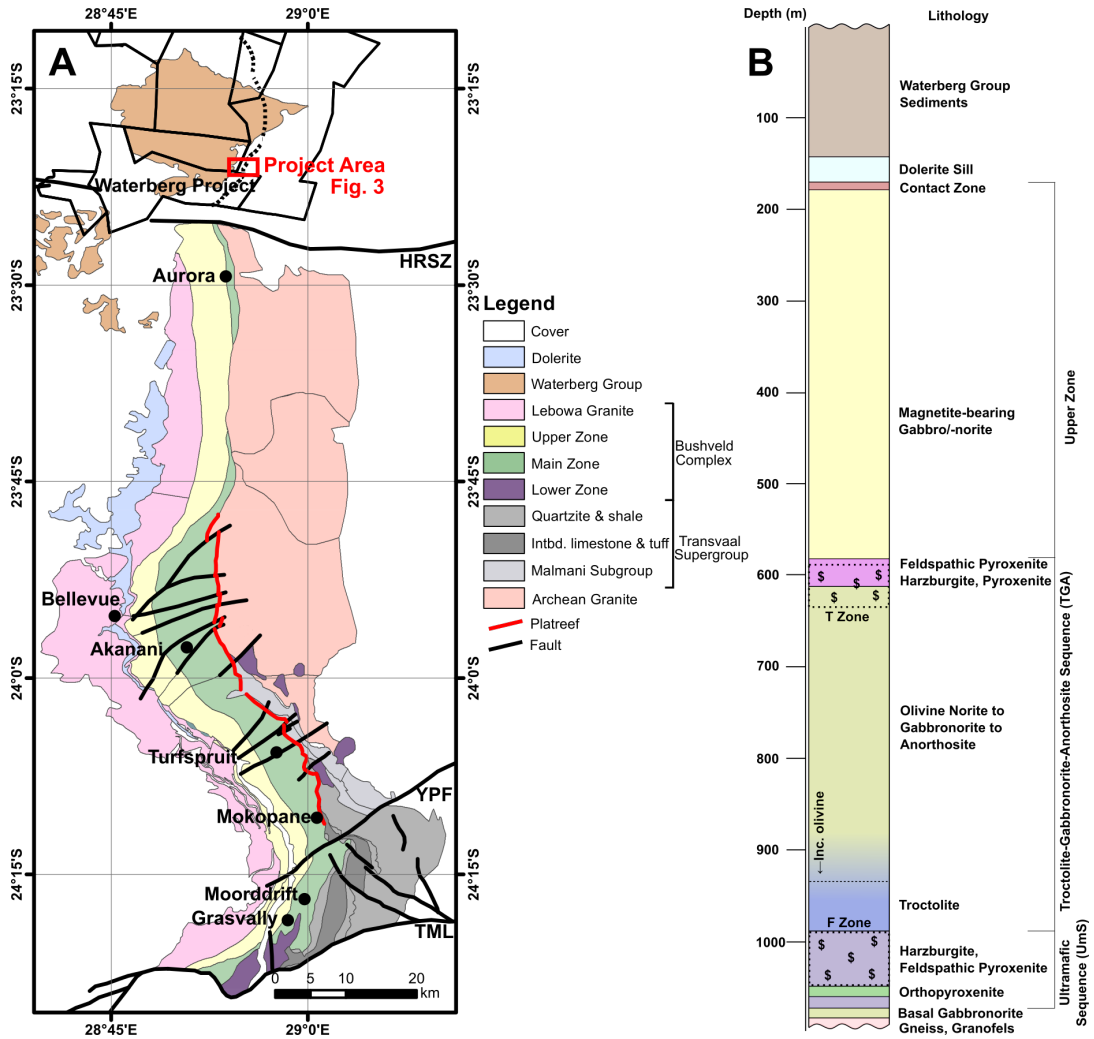


Figure 2: A: Geological map of the Northern Lobe of the Bushveld Complex showing the town of Mokopane and selected mining and exploration projects. HRSZ Hout River Shear Zone; YPF Ysterberg-Planknek Fault; TML Thabazimbi-Murchison lineament. Red Rectangle highlights the area of interest. B: Simplified stratigraphic column for the Waterberg succession. Both the basal gabbro-norite and the pyroxenite may not be present or occur at varying position and with varying thickness in the Ultramafic Sequence.

85 the noritic Marginal Zone, the Lower Zone comprising pyroxenites and harzburgites, the cyclical
 86 Critical Zone of chromitite–norite–pyroxenite, the Main Zone comprised of gabbro-norites and the
 87 Upper Zone of anorthosite, gabbro and magnetite. Lateral facies variations are common and
 88 not all zones are always present (Eales and Cawthorn, 1996; McDonald and Holwell, 2011). The
 89 Bushveld Complex is the world's most significant source of platinum-group elements including gold
 90 and chromite, as well as a source of magnetite and ilmenite (Lee, 1996).

91 2.1 The Northern Lobe and the Platreef

92 The geology of the Platreef and Northern Lobe are reviewed in great detail in Kinnaird et al. (2005),
 93 Ashwal et al. (2005), Kinnaird et al. (2005), McDonald and Holwell (2011) and Kinnaird and Nex
 94 (2015). and only aspects relevant to this contribution are discussed. An overview of the geology
 95 relevant for the discussion of the Waterberg Project is provided by Kinnaird et al. (2017).

96 The succession of mafic to ultramafic rocks in the Northern Lobe differs from the Eastern and

97 Western Lobes, ~~however~~ but all zones can be recognized. The Lower Zone was emplaced in trough-
98 like depressions and is characterized by high-Mg ~~whole-rock composition~~ rocks, chromitites and
99 zones of Ni-PGE mineralization ((Hulbert and von Gruenewaldt, 1982, 1985; Yudovskaya et al.,
100 2013b, 2017), ~~Yudovskaya et al., subm.~~). ~~It~~ The Lower Zone is separated from the Platreef by
101 older Transvaal sediments or granite gneisses. The ~~predominant~~ main basal unit is the Platreef,
102 a pyroxenite-dominated, lithologically variable unit irregularly mineralized with PGE₇ and Ni,
103 and Cu sulfides. It onlaps northwards onto progressively older Transvaal metasedimentary units
104 of oxide facies iron formations and dolomite and eventually onto Archean granites and gneisses
105 (Kinnaird et al., 2005). The Platreef disappears approximately half-way along the Northern Lobe.
106 ~~It is unconformably overlain by the Main Zone.~~ Data from Turfspruit confirms a general westward
107 dip of 30° to 60° close to surface, the dip however lessens with depth into a more regularly layered
108 sequence (Grobler et al., 2012; Yudovskaya et al., 2017). The Platreef is considered to be the
109 stratigraphic equivalent of the Critical Zone and unconformably overlain by the <2000 m thick
110 Main Zone. Overlying the Main Zone, the Upper Zone of the Northern Lobe is marked by the first
111 occurrence of massive magnetite (van der Merwe, 1976). The Upper Zone is transgressive and
112 overlies Main Zone for most of the strike length of the Northern Lobe, although in the north it is
113 in direct contact with a basement high (Fig. 2A). This basement high separates what might be a
114 southern magmatic basin comprising the Platreef, and a northern magmatic basin comprising the
115 Aurora mineralization (Kinnaird et al., 2005; McDonald et al., 2017). In the Bellevue drill core
116 (Fig. 2A), the Upper Zone comprises 1200 m of predominantly magnetite-rich olivine gabbro and
117 olivine ferrodiorite (Ashwal et al., 2005).

118 Correlations between the Eastern and Western Lobes and the Northern Lobe are complicated by
119 the enigmatic ~~†~~ Troctolite horizon Marker, ~~a c.~~ which is a ~110 m thick package of noritic troctolite
120 located 1100 m above the base of the Main Zone ~~located~~ along 35 km ~~of~~ strike length in the
121 central south of the Northern Lobe ~~of the Main Zone~~ (van der Merwe, 1976). Very little olivine
122 occurs in the Main Zones of the Eastern and Western Lobes (Eales and Cawthorn, 1996) and
123 recent findings research suggest that the ~~horizon~~ Troctolite Marker may be prospective for PGE
124 exploration (Tanner et al., 2014). ~~In contrast to the Eastern and Western Lobes, †~~ The Main Zone
125 of the Northern Lobe has an erosional contact at its base and is interpreted to significantly postdate
126 the emplacement of the Platreef (Holwell et al., 2005; Holwell and Jordaan, 2006). Rather than
127 being involved in the formation of the Platreef-equivalent Critical Zone deposits in the Eastern and
128 Western Lobes, the Main Zone of the Northern Lobe may therefore have retained its PGE budget
129 (Kruger, 2005; Seabrook et al., 2005). ~~rather than being involved with the formation of Critical~~
130 ~~Zone deposits (Kruger, 2005; Seabrook et al., 2005) and hence may have retained its PGE budget.~~
131 ~~While~~ Whereas most of the economic value of the Northern Lobe is concentrated in the Platreef,
132 sub-economic mineralization has been intersected in rocks interpreted to belong to the Main Zone
133 in the far north at Aurora and south at Moorddrift (Fig. 2A; Harmer et al., 2004; Manyeruke,
134 2007; Maier et al., 2008; Maier and Barnes, 2010; McDonald and Harmer, 2010; Holwell et al.,
135 2013; McDonald et al., 2017). ~~Overlying the Main Zone, the Upper Zone of the Northern Lobe is~~
136 ~~marked by the first occurrence of massive magnetites (van der Merwe, 1976).~~

137 ~~While generally overlying the Main Zone, the Upper Zone does directly overly a basement high in~~
138 ~~the northern part of the lobe, separating what might be called a southern “basin” with the Platreef~~
139 ~~and a northern “basin” with the Aurora mineralization (Kinnaird et al., 2005).~~

140 The Platreef is one of the world’s largest and most valuable ~~sequences~~ mafic to ultramafic succes-
141 sions ~~of~~ comprising platinum-group elements and associated significant Ni and Cu reserves (Nal-
142 drett, 2010). It differs from the UG2 and Merensky Reef deposits of the main Bushveld Complex

143 in terms of thickness of the package of being thicker, having lower average Pt/Pd ratios of approx-
144 imately 1 and lower grade of >4 g/t PGE where mined (Kinnaird et al., 2005). PGE and base
145 metal sulfides are generally associated, however in detail they may be decoupled, possibly due to
146 hydrothermal alteration and local remobilization (Kinnaird et al., 2005; Holwell and McDonald,
147 2006). A recent age date for the Platreef of 2056 ± 5 Ma (Yudovskaya et al., 2013a) overlaps within
148 error with a precise ~~2055-Ma~~ 2056.88 ± 0.41 Ma and 2057.04 ± 0.55 Ma ages for the Merensky
149 Reef (Scoates and Wall, 2015) and indicates that both deposits formed broadly contemporane-
150 ously. These ages are also in agreement with high-precision U-Pb dating indicating that indicates
151 crystallization of that the whole Bushveld Complex crystallized within over 1 Ma (Zeh et al., 2015).

152 Mineralization south of Mokopane at Moorddrift (Maier and Barnes, 2010), in the Aurora Project
153 (Harmer et al., 2004; Manyeruke, 2007; Maier et al., 2008; McDonald and Harmer, 2010; McDonald
154 et al., 2017) in the north of the Northern Lobe and in the Waterberg Project (Kinnaird et al.,
155 2014; Huthmann et al., 2016; Kinnaird et al., 2017; Kinnaird et al., ~~subm.~~) is explicitly excluded
156 from the Platreef (Kinnaird et al., 2005; McDonald and Holwell, 2011). The Aurora Project is
157 interpreted to be an upper Main Zone-hosted Cu-Ni-PGE deposit (McDonald et al., 2017) located
158 to the south of the Waterberg Project in the very northern end of the Northern Lobe (Fig. 2A).
159 At Aurora, the Main Zone reappears at surface and is in direct contact with Archean granite.
160 Mineralization occurs in two main mineralized horizons and a thinner discontinuous horizon closer
161 to the basal contact.

162 The Northern Lobe is separated from the Bushveld by the Thabazimbi-Murchison-Lineament. The
163 TML is a 500 km long and 25 km wide, ENE-WSW striking, long-lived and repeatedly reactivated
164 craton-scale structure (Good and de Wit, 1997). Based on seismic anisotropy, the TML is inter-
165 preted to represent a fundamental crustal and possibly deep lithospheric mantle breaklineament
166 within the Kaapvaal craton. ~~that~~ It is thought to have influenced regional stresses and tectonically
167 induced fluid flux during its reactive history between 2,960 and 145 Ma (Good and de Wit, 1997
168 and references therein). The stratigraphic correlation between the Northern Lobe to the north and
169 Eastern and Western Lobes to the south of the TML remains contentious (van der Merwe, 1976;
170 Ashwal et al., 2005; Kruger, 2005; McDonald et al., 2005; Kinnaird and Nex, 2015).

171 The Hout River Shear Zone (Fig. 2A) marks the boundary between the granulite-facies Southern
172 Marginal Zone (SMZ) of the Limpopo Complex and the stable Archean Kaapvaal Craton. ~~and~~ It
173 is generally interpreted to represent a composite structure along which the Southern Marginal Zone
174 was thrust southward during the Neoproterozoic (Smit et al., 1992; Barton et al., 2006). According
175 to recent work by Nicoli et al. (2015), the SMZ consists of reworked Kaapvaal Craton basement
176 gneisses, mafics, and clastic sedimentary rocks with ages between 3.3 and 2.7 Ga which are overlain
177 by younger sedimentary rocks. There is still little consensus regarding some elements of the
178 geodynamic history of the Limpopo orogeny (e.g. Treloar et al., 1992; Holzer et al., 1998; Barton
179 et al., 2006; Nicoli et al., 2015), however, a N-S directed long-lived tectonothermal activity of
180 more than 700 Ma is well established (Kramers and Mouri, 2011). Several studies (Schaller et al.,
181 1999; Barton et al., 2006; Clarke et al., 2009; Smirnov et al., 2013; Rajesh et al., 2014) proposed
182 a Paleoproterozoic (and not Archean) collision of the Zimbabwe and Kaapvaal craton that may
183 account for certain geological features observed in the project area. Regardless of the timing of
184 the Limpopo Belt orogeny, the location of the Waterberg Succession in the SMZ (~~instead of not~~ the
185 Kaapvaal Craton) may expose it to a level of Paleoproterozoic tectonism that ~~can~~ is not generally
186 ~~be~~ observed in the undeformed Bushveld Complex.

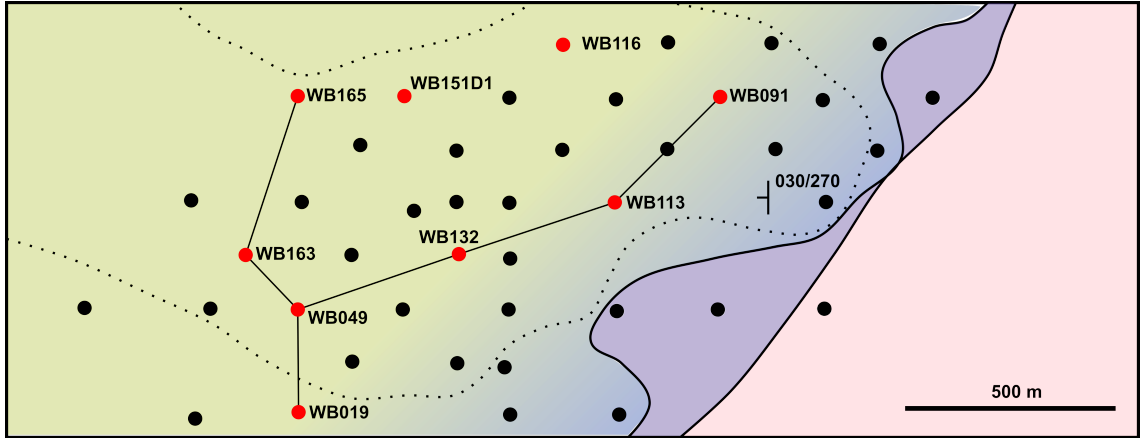


Figure 3: Close-up Subcrop map of the area of interest shown in Fig. 2. Shown are the positions of the drill holes investigated in detail (red) and the cross- and long-section drawn from Fig. 13 and 14. The stippled lines show marks the approximate outline of a 1 g/t 3E grade shell projected to surface. It has a 30 dip to the west. The sedimentary rocks overlying the succession are approximately 240 m thick in the east and their thickness increases slightly to the west. Shading indicates the changing depth of basement intersect from c. 600 m in the east to almost 1200 m in the west. Grid is 500 x 500 m N-S.

187 2.2 Local Geology

188 In the area immediately north of the Hout River Shear Zone (Fig. 2A) Platinum Group Metals
 189 (PTM) has intersected a mafic to ultramafic succession consisting subdivided into of an Ultramafic
 190 Sequence (UmS) overlain by what is now referred to as the Troctolite-Gabbronorite-Anorthosite
 191 Sequence (TGA) and an Upper Zone (UZ) of magnetite-bearing gabbroic rocks to ferrogabbros.
 192 The rocks are resting on a footwall of Archean gneisses that is commonly interfingering with pyroxenite
 193 (Fig. 2B). Except for one drill hole in the very south of the prospect, calc-silicate xenoliths
 194 are absent in the Waterberg area. Early pyroxenitic magmas intruding the floor rocks caused
 195 a melting and subsequent mingling of the two-component pyroxenitic magma and granitic melt,
 196 leading to the formation of a granofels. These earliest intrusion are envisioned as tube-like or
 197 chonolithic conduits that with subsequent intrusions were assimilated or broadened. The igneous
 198 rocks package of rocks are dipping e. $\sim 30^\circ$ toward the west-northwest, with variations due because
 199 to of structural controls and/or channel formation thermal-mechanical erosion. Significant faults
 200 are indicated by variations in intersection depth of the sedimentary-igneous rock contact, however,
 201 due to vertical drilling these potential steeply-dipping structures are not typically intersected.

202 Recent geophysical modeling suggests a continuation of the mafic succession to the north and west
 203 of the drill intersections and a greatly increasing thickness towards the southwest (Finn et al.,
 204 2015). The subdivision of the stratigraphy has changed since the early years of exploration and
 205 the ongoing work by company geologists and academics involved with this project has led to the
 206 questioning of some arrangements relationships (e.g. in Huthmann et al., 2016) and prompted a
 207 new subdivision to reflect interpreted petrogenetic relationships (Kinnaird et al., 2017).

208 The base of the succession may sometimes comprises very fine- to fine-grained orthopyroxenites
 209 and/or gabbronorites. Orthopyroxenites occur as cm- to meter-sized fragments to sill-like bodies
 210 that have sharp to gradational contacts with their respective host rocks and in places are almost
 211 completely assimilated by subsequent ultramafic rocks (see below). Gabbronorites generally appear
 212 less affected by their host and their relative age is uncertain. The pyroxenites are interpreted to
 213 be the crystallization product of initial liquid magmas to intruding the area and based on drill

214 intersects outside of the study area may intrude >100 m into the footwall granite-gneisses. Due to
215 very limited drilling into the deep basement, their distribution ~~however~~ is not certain. ~~and b~~Based
216 on the observed degree of assimilation and their distribution, they may also represent autoliths.
217 The gabbro-norites, on the other hand, are plagioclase-dominated rocks of varying grain-size (finer-
218 grained towards the footwall) that ~~in thin section~~ resemble the ~~geology of~~ gabbroic rocks observed
219 higher up in the succession.

220 Harzburgites and feldspathic pyroxenites of the UmS are the primary basal unit of the succession.
221 ~~Where present~~The UmS is discontinuous and where present, ~~the package~~it may exceed 80 m in
222 thickness, hosts PGE and Au mineralization and unevenly distributed chromite clusters and seams.
223 Olivine-bearing units in the UmS are very strongly altered with ~~often only~~ relicts of primary
224 minerals remaining, having been replaced primarily by serpentine and magnetite. ~~Calc-silicates~~
225 ~~are absent, however~~†The unit is very heterogenous and comprises small amounts of juxtaposed
226 pyroxenite, serpentinite, troctolite and dunite. ~~Calc-silicates xenoliths are absent.~~

227 Overlying the UmS, the TGA Sequence is primarily composed of gabbro-noritic rocks with minor
228 anorthosites, grading into norites, olivine norites and troctolites at ~~it~~the base (Fig. 2B). The
229 rocks appear to ~~be~~ grade into the UZ at the top of the succession. ~~and d~~Due to the fine-grained
230 nature of the magnetite and similarity of rock types, no clear contacts can be observed. The
231 enigmatic troctolites, ~~which are dissimilar to any ultramafic Bushveld units,~~ have a gradational,
232 mingled or irregular contact with olivine gabbro-norite upwards and a sharp, erosional(?) contact
233 with harzburgite at the base (Fig. 4B). Further south, the top of the TGA Sequence is host to
234 the T Zones, a set of 2 to 3 ~~discontinuous, mineralized~~ gabbro-norite~~ie~~, pyroxenite~~ie~~ to troctolite~~ie~~,
235 ~~discontinuous, mineralized~~ horizons. In the area of focus for this study the T Zones are either
236 absent or extremely poorly developed, possibly related to non-deposition, structural controls, or
237 erosion preceding the deposition of Waterberg Group sediments.

238 The upper part of the ~~succession on the~~ Waterberg Prospect is composed of magnetite-bearing gab-
239 bro-norite and gabbro, that ~~contain~~have varying ortho- and clinopyroxene contents. It is tentatively
240 correlated with the Upper Zone elsewhere in the Complex, even though it lacks the magnetite
241 layers ~~which~~that are characteristic for the Upper Zone elsewhere in the Bushveld Complex (e.g.
242 Molyneux, 1974; Ashwal et al., 2005). Instead, magnetite in the Upper Zone at the Waterberg
243 Project occurs as very fine-grained disseminations that in the field are most easily identified by the
244 use of a magnetic susceptibility meter. The UZ thins in places and its exact distribution requires
245 further research ~~and may be controlled by structure-controlled blocks and erosion. The absence~~
246 ~~of distinct magnetite layers and more evolved apatite-bearing rocks may be related to erosion of~~
247 ~~more evolved units rather than non-deposition.~~

248 The top contact of the Waterberg Succession is a remarkably flat erosional unconformity overlain
249 by Paleoproterozoic Waterberg Group sediments (Callaghan et al., 1991; Huthmann et al., 2016),
250 typically starting with a ~~coarse, poorly-sorted~~basal and polymict breccia. The top of the succession
251 is complex and sometimes an up to 10 m wide and strongly altered, sheared and tuffaceous contact
252 zone is located between the sediments and igneous units. Detrital zircons of the basal breccia have
253 recently been dated and encompass age clusters of 2045 to 3354 Ma, generally attributed to the
254 Limpopo Belt (Corcoran et al., 2013; Huthmann et al., 2016).

255 Recently acquired age dates (2059 ± 3 and 2053 ± 5 Ma; Huthmann et al., 2016) from zircons
256 extracted from mafic rocks of the succession are within error coeval with published ages for the
257 Eastern and Western Lobe of the Bushveld Complex (Walraven and Hattingh, 1993; Walraven,
258 1997; Buick et al., 2001; Scoates and Friedman, 2008; Scoates and Wall, 2015; Zeh et al., 2015),

259 and the Northern Lobe (Yudovskaya et al., 2013a), ~~and suggest~~ which indicates that the intrusions
260 ~~are related~~ belong to the Bushveld Large Igneous Province and are therefore related.

261 Mineralization occurs in ~~two mineralized zones~~ the T and F zones, located just below the Up-
262 per Zone and in the Ultramafic Sequence, respectively (Fig. 2B). ~~The~~ ~~The so-called T and F~~
263 ~~Zones~~ mineralized zones are 3 to >60 m thick and have so far been intersected along 17 km of strike
264 (Kinnaird et al., 2014). T and F Zone refers to zones of elevated PGE grades which in detail are
265 ~~not not~~ strictly stratabound (2B). The T Zone in particular occurs in two distinct stratigraphic
266 levels with distinct mineralogy (Kinnaird et al., 2017). New mineral assemblages are still being dis-
267 covered and will be subject of upcoming publications. The mineralized F Zone closely follows the
268 westerly trend of the harzburgite chonoliths and may form “Super F Zones” with grades that can
269 exceed 15 g/t 3E (Pt+Pd+Au) in individual assayed intervals ~~and that have no direct analogue in~~
270 ~~the Bushveld Complex~~ (Kinnaird et al., 2017). These zones of high grade are separated by weakly
271 to ~~non-un~~ mineralized ~~rock~~ troctolite of the TGA Sequence.

272 3 Methodology

273 For this study ~~drill core from~~ nine holes intersecting the center and periphery of one of the Super F
274 (mineralized) Zones (Fig. 3) have been logged. The selected drill holes allow for an assessment of
275 any correlation of rock types, distribution of the mineralization and ultimately the generation of an
276 emplacement model. This particular Super F Zone forms an elongated, SW-plunging mineralization
277 envelope of >200 by >1000m with ~~highly~~ anomalous PGE and Au of greater 0.5 g/t ~~values~~ over
278 more than 120 m in core and economic grade of over 2.5 g/t over more than 60 m. ~~PTM’s~~ Platinum
279 Group Metal’s assay database for the study area, consisting of approximately 9500 assays of Pt,
280 Pd, Ni, Cr, Cu, Co and S, ~~assays~~ was made available. Figures 13 and 14 show typical long and
281 cross sections through this zone and assays ~~as per~~ derived from PTM’s database.

282 Fifty-eight samples of approximately 25 cm long, NQ size, quarter-core samples were selected
283 from the logged drill holes. Care was taken to avoid zones of veining, strong alteration and au-
284 tooliths/xenoliths. Sample preparation was conducted at the University of Witwatersrand following
285 established methods (Wilson, 2012).

286 All samples were analyzed for major and trace elements and loss on ignition (LOI) at the University
287 of the Witwatersrand analytical facilities. Major and selected trace elements were determined using
288 a Panalytical PW2404 X-ray fluorescence (XRF) spectrometer with fused disks and the SuperQ
289 program. Sulphur was determined for selected samples from pressed pellets employing the same
290 instrument and the ProTrace program. All other trace elements were determined by inductively
291 coupled plasma mass spectrometry (ICP-MS) employing a Perkin Elmer Elan instrument. All
292 analytical procedures followed the methods described by Wilson (2012).

293 Platinum group elements and Au were determined for selected samples at Cardiff University from
294 15g sample weight powders prepared at the University of the Witwatersrand. The analysis was
295 carried out by Ni-sulphide fire assay followed by Te co-precipitation and ICP-MS (Huber et al.,
296 2001; McDonald and Viljoen, 2006). Accuracy for all whole-rock geochemistry was constrained by
297 the analysis of certified international reference materials and internal standards while the precision
298 for fire assays was estimated by repeat analysis of several samples (see supplementary data).

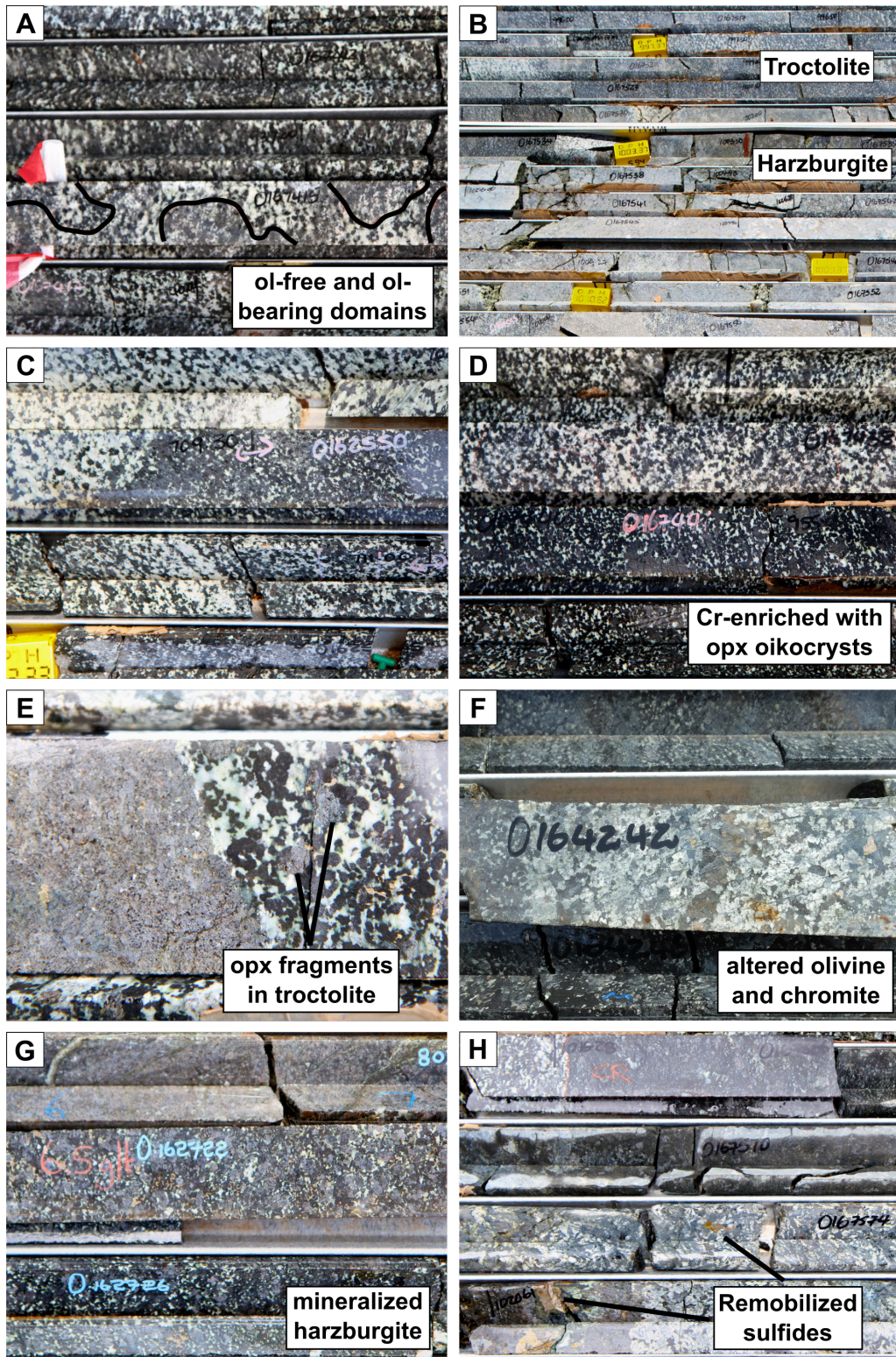


Figure 4: Textural relationships in examples of rock types from drill core observed in the Waterberg Project. A: Upper contact of the TGA Sequence troctolite showing discrete zones of gabbroic and troctolitic rocks interpreted to represent mingling of cumulates; B: Typical Ultramafic Sequence. In the top tray the sharp contact between overlying troctolite and harzburgite is visible; C: Variations in the troctolite zone showing leucotroctolite and zones of abundant orthopyroxene oikocrysts; D: Variations in olivine abundance in the troctolite zone. The oikocryst-rich melatroctolite is characterized by significant spikes in Cr content; E: Orthopyroxenite autolith in troctolite. Note the small pyroxenite fragments in the troctolite and the presence of possibly remobilized sulfides in both rocks; F: Chromite in TGA Sequence troctolite adjacent to an alteration halo and remobilized sulfides; G: Mildly altered mineralized zone with 6.5 g/t Pt+Pd+Au; H: Vari-textured zone of Cr-enriched serpentinite and large sulfide blebs remobilization.

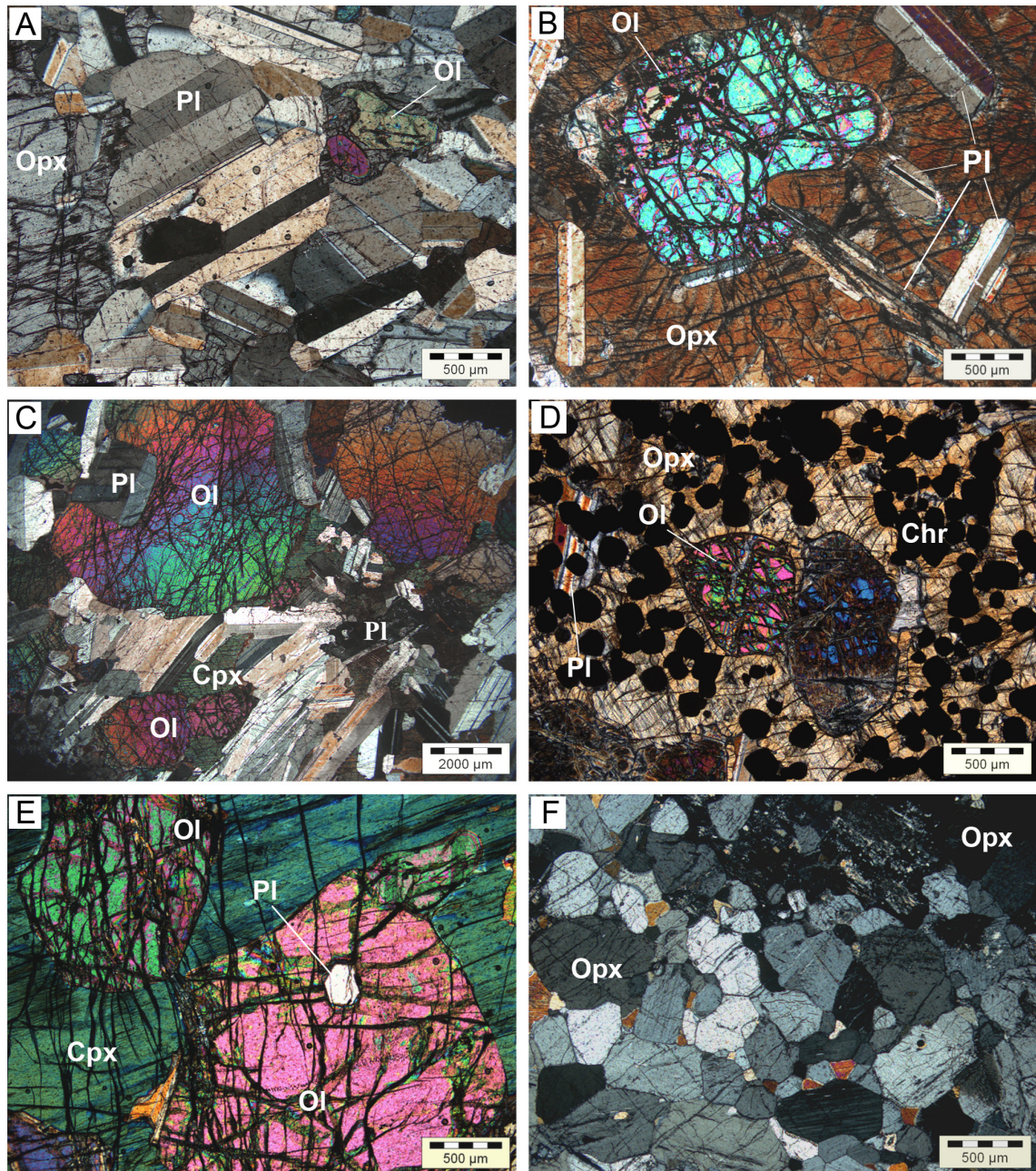


Figure 5: Rock textures of the Waterberg body under cross-polarized transmitted light. A: Small olivine *crystals* rimmed by peritectic orthopyroxene in olivine-bearing leuconorite in the uppermost part of the TGA Sequence; B: Corroded olivine and euhedral plagioclase laths in orthopyroxene oikocryst in olivine norite; C: Coarse olivine and plagioclase of smaller size in troctolite; D: chadacrysts of olivine and chromite enclosed by orthopyroxene in poikilitic chromitite of the Ultramafic Sequence; E: Coarse grains of olivine with plagioclase inclusions among interstitial clinopyroxene in lherzolite of the Ultramafic Sequence; F: Recrystallized orthopyroxenite with triple junction texture of orthopyroxene grains.

299 4 Results

300 4.1 Field relationships and petrography

301 Given the *very heterogeneous and irregular nature of lithologies observed in drill core, complexities*
 302 *of the Waterberg area and the high probability of non-sequential intrusion of cumulates, some of*

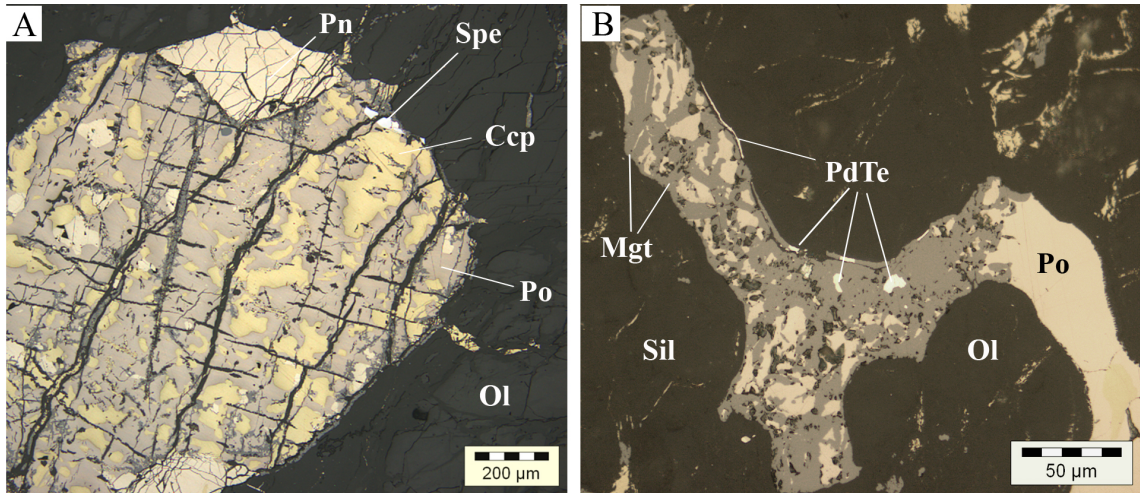


Figure 6: Sulfide assemblages of the F Zone under reflected light. A: Primary magmatic sulfide bleb composed of pentlandite (Pn), pyrrhotite (Po) and chalcopyrite (Ccp) in harzburgite. Sperrylite (Spe) occurs at the margin on contact with olivine (Ol); B: Interstitial pyrrhotite partly replaced by secondary magnetite (Mgt) in harzburgite. Kotulskite (PdTe) is located inside magnetite and remobilized along the contact between sulfides and silicates (Sil). Olivine is completely replaced by serpentine.

303 ~~the complexities have been simplified and we discuss~~ suites of intrusives and zones of mineralization
 304 rather than individual lithologies ~~are discussed~~ (cf. McDonald and Holwell, 2011). It has to be
 305 emphasized, that ~~while~~ although individual rock types are important, the amount of variation in
 306 mineralogy, alteration, chemistry and mineralization makes lithological correlation between 200 m-
 307 spaced drill holes ~~incredibly difficult on a lithology level~~. The variation in mineralogy observed in
 308 the core may be related to mingling and mixing of crystal-rich liquids. The term mixing is used in
 309 situations where two or more magmas produce hybrid rocks with the identities of the parent mag-
 310 mas obscured, whereas mingling represents interactions in which the original magmas or cumulates
 311 retain their identity (Fig. 4; Wiebe, 1980). ~~As outlined earlier, the succession is subdivided into~~
 312 ~~Upper Zone (poorly developed in the study area), Troctolite-Gabbronorite-Anorthosite Sequence~~
 313 ~~and Ultramafic Sequence.~~

314 In accordance with informal tradition amongst Bushveld Complex geologists, rock types are named
 315 based on their cumulus mineralogy, hence a rock consisting of cumulus olivine and plagioclase with
 316 significant intercumulus orthopyroxene is called a troctolite rather than a olivine norite. The term
 317 reef is avoided in favor of mineralized zone, as reef implies a lateral continuity that may not be
 318 present in the Waterberg Succession. Additionally, the mineralization may ~~to a limited degree~~
 319 ~~transgress rock type boundaries to a limited degree.~~ boundaries between rock types.

320 The following section provides drill core and petrological observations for the four main lithologies
 321 of the study area, namely the basal orthopyroxenite and gabbronorite, as well as the Ultramafic
 322 Sequence (UmS) and Troctolite-Gabbronorite-Anorthosite Sequence (TGA).

323 4.1.1 Marginal Basal orthopyroxenite

324 Orthopyroxenite occurs as sill-like bodies and as autoliths throughout the ~~lower part~~ Ultramafic
 325 Sequence and more rarely in the troctolite- ~~of the TGA Sequence of the succession, generally in~~
 326 ~~troctolites and harzburgites~~. Outside the area investigated as part of this study, orthopyroxenites
 327 may intrude deep into the footwall, however, due to limited drilling into the basement, ~~it~~ their

328 detailed distribution is not well ~~resolved~~ established. The autoliths are several centimeters to <6
329 m in size. ~~Their with generally well recognizable~~ contacts are generally well-recognizable, but
330 particularly in harzburgite may be obscured by alteration. ~~which may be obscured by alteration,~~
331 ~~particularly in the harzburgites.~~ The rocks consist of medium to very fine-grained orthopyroxene
332 and may contain up to 15% olivine. Clinopyroxene and plagioclase are minor interstitial phases.
333 Both orthopyroxene and olivine may host disseminated crystals of chromite which range in size
334 from <50 μm to <10 μm . The smallest of those crystals may form trails in the host silicate.

335 The orthopyroxenites are barren, or, where their texture suggests sulfide remobilization into the
336 rock, contain low trace 3E (Pt+Pd+Au) grade levels. Inspection of the drill cores indicates ~~that that~~
337 ~~where Cr is elevated in the assays, lithologies are often orthopyroxenites or orthopyroxene-rich~~ intervals
338 of orthopyroxenite often have highly anomalous Cr values (Fig. 13 and 14, see below). Core logging
339 also ~~suggests~~ indicates that incorporation of these pyroxenites by younger olivine-bearing rocks may
340 lead to zones of increased orthopyroxene oikocrysts or xenocrysts with chromitite clusters.

341 ~~The rocks consist of medium to very fine-grained orthopyroxene and may contain up to 15% olivine.~~
342 ~~Clinopyroxene and plagioclase are minor interstitial phases. Both orthopyroxene and olivine may~~
343 ~~host disseminated crystals of chromite. Observed crystals range in size from <50 μm to <10 μm~~
344 ~~and for the smallest crystals can form trails in the host silicate.~~

345 Near the granite-gneiss footwall contact, varying amounts of interaction between ~~the rocks~~ magmas
346 can be observed, ~~and the drill core shows features~~ ranging from discrete felsic and pyroxenitic
347 patches to almost complete homogenization. ~~While~~ Although the amount of pyroxenite preserved
348 in the core is often limited to patches of cm-size, a generally decreasing crystal size up hole can be
349 observed. The respective thin sections have small crystal size, triple-junction assemblages of or-
350 thopyroxene, and occurrences of quartz-feldspar granophyric intergrowths. Fragments of orthopy-
351 roxenite with fine-grained granoblastic texture can be found in ultramafic assemblages, indicating
352 their assimilation by later melt influxes. Together, these observations indicate that the pyroxenite
353 was the first unit to intrude the study area.

354 4.1.2 Marginal Basal gabbronorite

355 The term marginal gabbronorite is used to refer to occurrences of gabbroic to anorthositic rocks
356 of centimeter to meter thickness found close to the base of the succession. The rocks are very fine-
357 to medium-grained, dark in color and when fine-grained resemble pyroxenites in hand specimen.

358 Thin sections show that the dark color is due to extensive cloudiness and spotty alteration of
359 plagioclase. The basal rocks exhibit highly variable textures both within a single thin section as
360 well as between different drill cores. Modal mineralogy is dominated by plagioclase with varying
361 amounts of clino- and orthopyroxene. Pyroxene may occur interstitial, as small cumulus crystals
362 or as large oikocrysts. Plagioclase is often altered by very fine-grained mineral aggregates. Overall,
363 in thin section these rocks resemble gabbroic rocks higher up in the stratigraphy.

364 4.1.3 The Ultramafic Sequence

365 The mineralized Ultramafic Sequence (UmS) ~~in the project area~~ is a highly complex array of a
366 variety of rock types that includes strongly to very strongly altered harzburgite, ~~troctolite~~, serpen-
367 tinite ~~and~~, feldspathic pyroxenite and minor troctolite with very fine to pegmatitic crystal size.
368 It varies in thickness between 60 and >80 m and generally comprises autoliths of orthopyroxenite

369 which may or may not be altered and which do not contain primary sulfides. Alteration and re-
370 mobilization appear to have at least some control over the high grade zones and may have affected
371 low grades zones as well (Fig. 4H). Chromite may occur as highly irregularly-distributed seams or
372 clusters of chromite grains that can not be correlated between the widely-spaced holes.

373 The UmS is the major basal unit of the the Waterberg Succession and can be recognized by its
374 strong alteration and overall heterogenous texture. Its texture which are is in sharp contrast to
375 the overlying troctolite's "salt and pepper" appearance texture (Fig. 4B). The lower contact of the
376 UmS may be with either with the marginal units, with granofels, or, at the outer margins of the
377 mineralized zone with barren, relatively unaltered meso- to melatroctolite (Figs. 13 and 14). The
378 appearance of an the unaltered texture in of the troctolite invariably indicates barren zones (Fig. 13,
379 WB113D0), however sulfide remobilization may lead to irregular low grade zones—zones of highly
380 irregular grade (Figs. 4H, 13, WB091D0). Due to this, base metal sulfides can be found highly
381 concentrated and may comprise zones of >10 g/t 3E for individual samples (Fig. 4H bottom). This
382 relationship is not consistent, however, and both base and previous metals may occur separately.
383 Where drill cores suggest interactions of different magmas, base metal sulfides (and associated
384 PGE) may be absent (Fig. 4H top).

385 In thin section The harzburgites are medium- to coarse-grained rocks consisting of about equal
386 proportions of orthopyroxene and olivine. Plagioclase and clinopyroxene are minor interstitial
387 components. Plagioclase may form leucocratic patches of generally finer grain size. Pyroxene and
388 olivine, in particular, are very strongly altered and only the outline of former minerals remains
389 in some cases. The dominant alteration is to serpentine plus and magnetite, however, chlorite and
390 a range of other alteration minerals occur. Carbonates or carbonate overprint are not observed.
391 Chromite forms rare small grains in amounts of less than 1 vol%, although it can be found as
392 chromite clusters (Fig. 5) or as irregular seams. Sulfide minerals observed as part of the F Zone
393 mineralization include pentlandite, pyrrhotite and chalcopyrite, often associated with significant
394 secondary magnetite due to the strong alteration of the harzburgites. The P platinum group min-
395 erals are variable in the T Zone are variable (Fig. 6). with dominant Ssperryllite is dominant and
396 and subordinate Pt-Pd bismutho-tellurides, Au-Ag alloys, Pd arsenides and Pt-Rh sulpharsenides
397 can be found.

398 4.1.4 The TGAroctolite-Gabbronorite-Anorthosite Sequence

399 The troctolites in the lower part of the Troctolite-Gabbronorite-Anorthosite (TGA) Sequence form
400 an unmineralized, 50 to 110 m thick package ranging in composition from leucotroctolite and olivine
401 norite to melatroctolite and with rare plagioclase towards the base. The troctolites have a cross-
402 cutting and erosional relationship with underlying harzburgites of the UmS (Fig. 4B). Towards
403 the lower contact, the troctolite typically gradually increases in olivine content and its appearance
404 is more homogeneous. Most of the sequence contains between 50 and 80% olivine, giving it a
405 distinct salt and pepper appearance. Sharp breaks in composition may occur, however, leading
406 to the juxtaposition of rocks of varying olivine content (Fig. 4C). Where developed, the more
407 anorthite-rich phases appear to crosscut and postdate the olivine-rich zones, perhaps indicating
408 fractionation. The sequence is coarse-grained with rare pegmatitic patches, typically with increased
409 anorthite content. Most of the sequence contains up to 10% orthopyroxene in the form of up
410 to several centimeter-sized oikocrysts. This may increase in the lower half of the sequence to
411 >40%, usually at the expense of plagioclase. The upper 10 to 50% of the sequence may be very
412 heterogeneous in composition and discrete domains of troctolitic and gabbronoritic composition

413 can be distinguished (Fig. 4A). This is interpreted to indicate the interaction of the respective
414 differentiating crystal-rich liquids.

415 As with the Theharzburgite of the UmS, the troctolite is host to a number of pyroxenitic autoliths
416 ranging in size from a few centimeters to several meters. The autoliths are typically medium- to
417 coarse-grained, dominated by orthopyroxene and with sharp, cusped contacts. They may display a
418 pronounced enrichment in Cr independent of their visible mineralogy (Fig. 4E, see below). Where
419 visible chromite crystals are absent, chromite can be found as inclusions in silicate phases. This
420 Cr enrichment can also be recognized in PTM's assay intervals comprising troctolite and autoliths
421 (Fig. 13 and 14). The intrusion and emplacement of hot, olivine-phyric silicate liquids into
422 earlier orthopyroxenites is thought to have led to their thermal-erosion, transport,
423 and incorporation of orthopyroxenite into younger melt fluxes thereby leading to anomalous Cr
424 contents.

425 In thin section, the troctolites are characterized by cumulate textured olivine and plagioclase and
426 strong alteration of both minerals. Depending on the sampling location, the sample may contain
427 significant amounts of oikocrystic orthopyroxene and very limited plagioclase (Fig. 5). All major
428 mineral phases may host <50 μm crystals of chromite, often rimmed by magnetite.

429 Gabbronorites make up the largest part of the TGA Sequence. They form a unit of 100 to 300 m
430 thickness, consisting of varying amounts of orthopyroxene, plagioclase and clinopyroxene. Varia-
431 tions in pyroxene content may bring this unit close to a norite composition, while varying amounts
432 of olivine may occur at the base where the rocks grade into troctolite. This transition usually in-
433 volves an increase in olivine content with what appears to be a mingling of gabbroic and troctolitic
434 material, often forming discrete areas in core. The unit is generally medium-grained, however rare
435 pegmatoidal patches of gabbroic composition occur. In the southern half of the Waterberg Project
436 the upper TGA Sequence may host a sometimes pegmatoidal, mineralized zone of anorthositic,
437 pyroxenitic, noritic to troctolitic composition (the T Zone). In the study area, these rocks are
438 absent or poorly developed with PGE and Au only weakly elevated (Fig. 14, WB165D0). The
439 controls on the deposition or emplacement of the mineralization are currently unresolved and either
440 non-deposition/emplacement or later erosion appear plausible.

441 In thin section, the gabbronorites are typical gabbroic cumulate rocks consisting of coarse plagioclase
442 and varying amounts of clino- and orthopyroxene. The latter two may occur as oikocrysts.
443 Upwards through the stratigraphy the amount of clinopyroxene is generally increasing and sporadic
444 inverted pigeonite may be observed. while aAlteration throughout the whole sequence is generally
445 limited minor. The pyroxenes may occur as oikocrysts. Inverted pigeonite may be observed in this
446 zone, however its occurrence is only sporadic.

447 In other parts of PTM's prospects, the TGA Sequence is overlain by magnetite-bearing gabbros
448 and gabbronorites of the Upper Zone. In the study area, however, these rocks are poorly developed
449 to absent. Due to the fine-grained, disseminated nature of the magnetite in the Upper Zone, the
450 contact can be hard to identify in core and a sharp decrease in magnetic susceptibility due to the
451 appearance of magnetite is taken as the contact.

452 4.2 Geochemistry

453 4.2.1 ~~Variation diagrams~~ Major and trace element variation diagrams

454 Data are displayed as bivariate plots with MgO as the differentiation index in Figs. 7 and 8.
455 Variations in major element compositions (Table 1) for the rocks analyzed reflect the proportion of

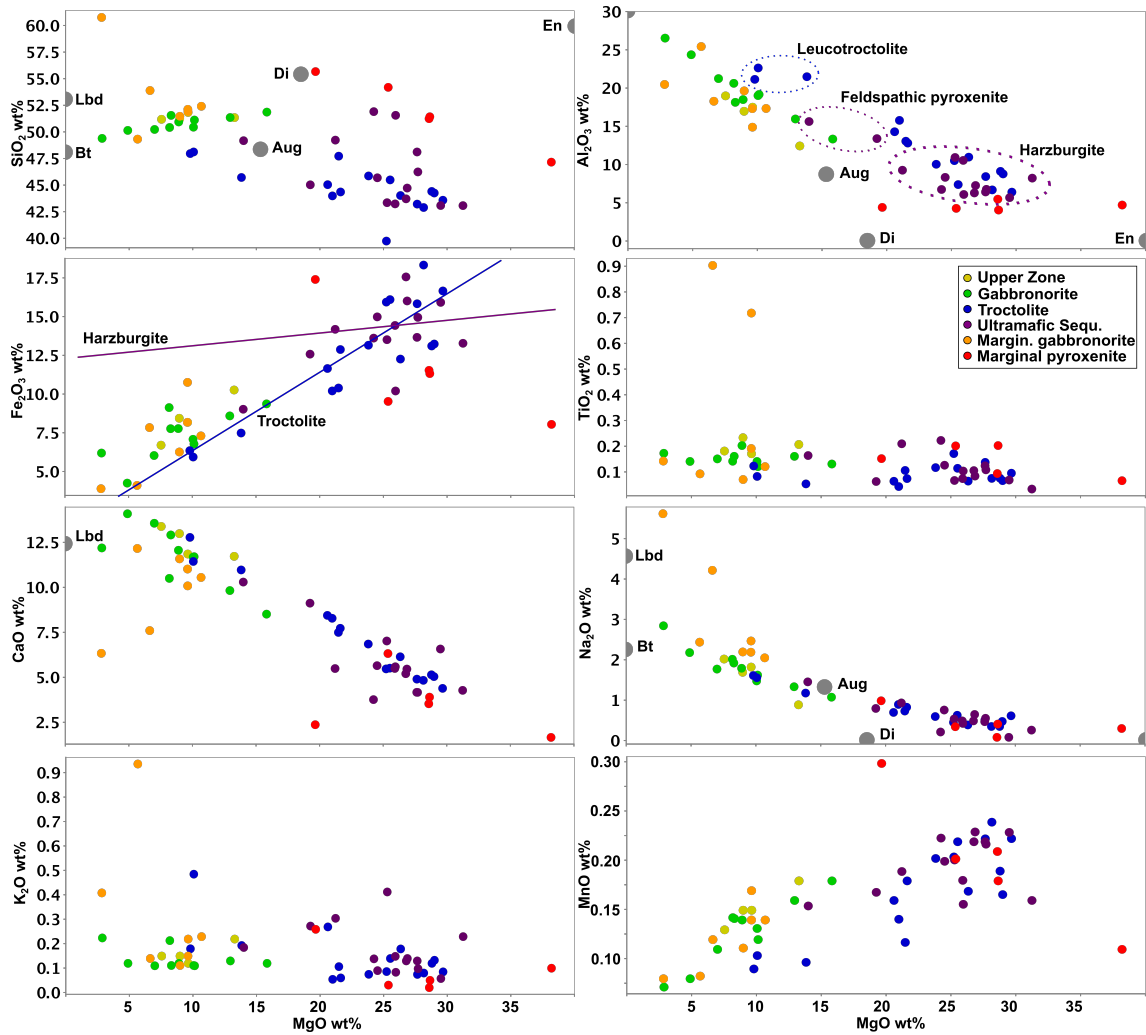


Figure 7: Binary variation diagrams of MgO vs major elements. Except for two samples of feldspathic pyroxenite, the UmS group of samples comprises only harzburgite. The lines in the SiO_2 vs. Fe_2O_3 plot demonstrate the different trends of troctolite and harzburgite (see text). Lbd Labradorite; Bt Bytownite; Aug Augite; Di Diopside; En Enstatite.

456 olivine, pyroxene and plagioclase present and clearly differentiate between the mostly olivine-and
 457 + orthopyroxene-dominated Ultramafic Sequence and the plagioclase + clinopyroxene ± olivine ±
 458 orthopyroxene and plagioclase assemblages of the TGA Sequence and Upper Zone (Fig. 7; Table
 459 1). Exceptions are three plagioclase-rich (leuco-) troctolite samples which plot towards lower Mg
 460 values. Data are displayed as bivariate plots with MgO as the differentiation index in Figs. 7 and
 461 8.

462 The rocks have SiO_2 values ranging from 40 to 61 wt% with a and decrease towards higher MgO.
 463 Three groups of samples can be distinguished: i) harzburgites and 2 feldspathic pyroxenite samples
 464 of the UmS form a high-Mg cluster of samples; ii) MarginalBasal orthopyroxenites form a separate
 465 trend from other samples; iii) rocks of the TGA sequence and UZ, dominated by troctolites and
 466 gabbronorites and troctolite, form a trend extending from high- to low-Mg rocks. The wide range
 467 of MgO and other major elements for some of the troctolites reflects their cumulus assemblage
 468 ranging from dunite < 90% olivine to leucotroctolite (Fig. 7).

469 The orthopyroxenites follow a trend of higher SiO_2 for a given MgO than the harzburgites. This
 470 elevated SiO_2 reflects the higher SiO_2 in orthopyroxene assemblages. Al_2O_3 follows a sharp, de-

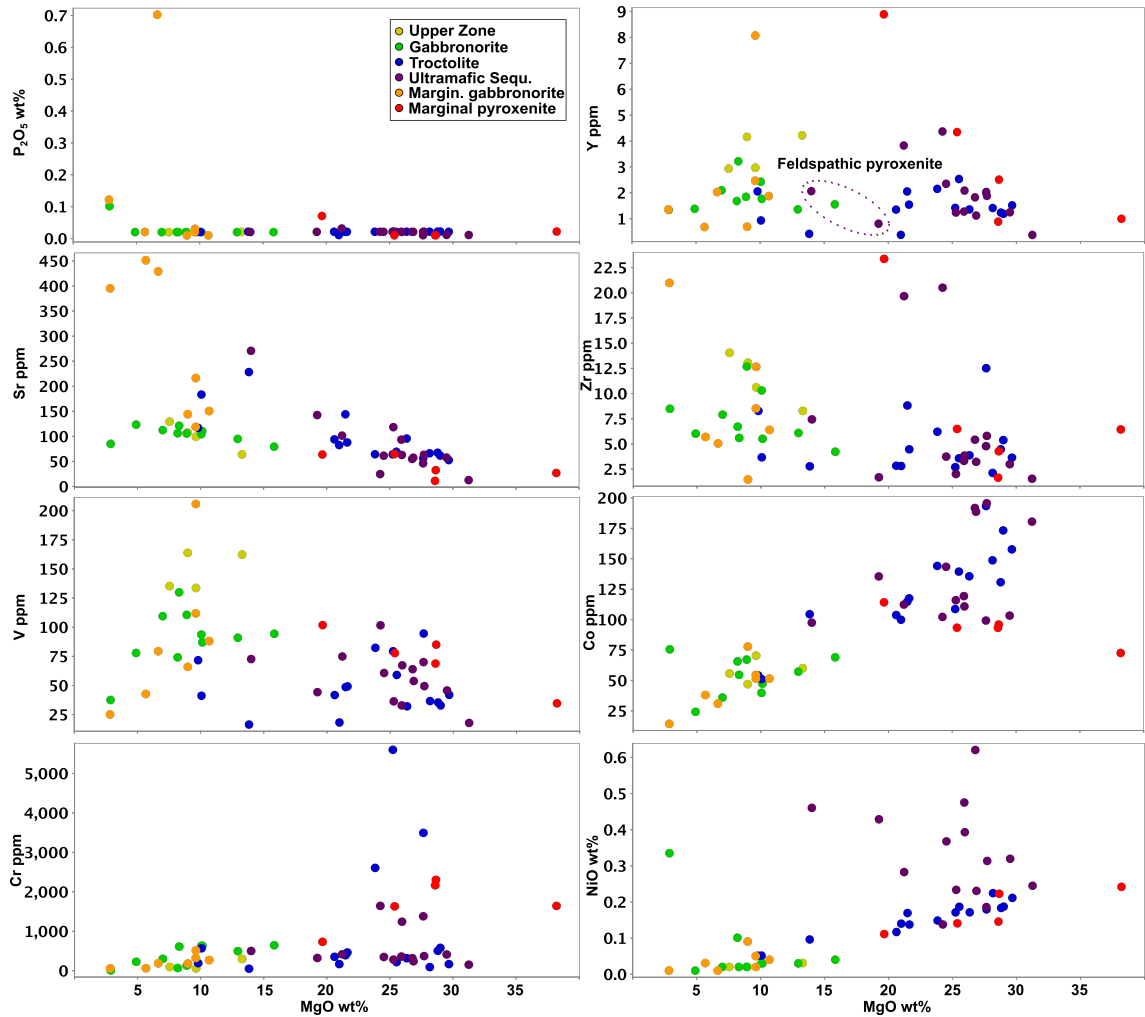


Figure 8: Binary variation diagrams of MgO vs trace elements.

471 creasing trend with values between 4 and 27 wt%. Fe_2O_3 (as total Fe) decreases with decreasing
 472 MgO for most samples, even though there are Mg-rich, orthopyroxenite outliers. Trend lines drawn
 473 for the troctolites and harzburgites show that the rocks types follow slightly different trends (Fig.
 474 7). Low Fe_2O_3 values correspond to the paucity of magnetite in the study area. CaO and Na_2O
 475 increase with decreasing MgO, reflecting the plagioclase and pyroxene assemblages of the Upper
 476 and Main Zones and TGA Sequence. K_2O is generally low with most rocks having values
 477 0.1 and 0.2 wt%. P_2O_5 is less than 0.1 wt% reflecting the absence of apatite even in the Upper
 478 Zone. TiO_2 values are low, again corresponding to limited development of the Upper Zone.

479 ~~Gabbronorites and ferrogabbros belonging to the TGA Sequence, Upper Zone and the marginal~~
 480 ~~gabbronorites are characterized by low Fe_2O_3 and elevated Al_2O_3 and Na_2O .~~ V strongly frac-
 481 tionates into magnetite and hence values are higher for Upper Zone samples. NiO is enriched in
 482 troctolites, olivine-bearing pyroxenites and due to the presence of sulfides strongly anomalous in
 483 mineralized rocks due to the occurrence of sulfides. Cr is strongly enriched in samples containing
 484 clusters of chromite, i.e. certain pyroxenites and troctolites that contain small chromite clusters.
 485 Incompatible P_2O_5 , Sr and Zr element levels are low in general and their pattern may be influenced
 486 by host rock and footwall assimilation for some of the units with outliers for the basal gabbronorite
 487 (Fig. 8).

488 4.2.2 Multi-element normalized plots

489 All samples analyzed show almost identical trends on primitive mantle normalized multi-element
490 plots (Sun and McDonough, 1989). They display negative Th, Nb, Ta and sometimes mildly
491 negative Rb and Ti anomalies while in most cases displaying strong positive Sr and Eu anomalies
492 (Fig. 9). Gabbroic rocks display $Rb < Ba$, while the opposite is true for the harzburgites and
493 marginal pyroxenites. Mean Rb/Ba_N for the troctolites is 1.

494 For most groups of samples MREE and HREE are depleted relative to primitive mantle values.
495 Eu/Eu^* ranges from 1.1 to 2.1, HREE are generally not fractionated with mean Tb/Yb_N of close
496 to 1. The marginal pyroxenites display significant variation in and have a mean Tb/Yb_N of 1.6
497 (Fig. 10). LREE are enriched (Mean $Ce/Sm_N = 2$) with mean Ce/Sm_N for the TGA Sequence and
498 basal gabbronorites at 2.7 and 2.2 respectively. Th is enriched relative to Sm, in particular in the
499 troctolites and marginal pyroxenites (Mean $Th/Sm_N = 4.2$ and 3.4, respectively). WhileAlthough
500 low Eu abundances are expected for the plagioclase-poor pyroxenites, there is some decoupling of
501 plagioclase mode and Eu anomalies.

502 Samples of UZ, TGA Sequence gabbronorite and troctolites display a tight grouping of analysis
503 results with patterns that are almost identical. whereas†The marginal pyroxenites, mineralized
504 harzburgites and basal gabbronorites display more within-group variation while still following the
505 overall pattern. Maximum within-group variation is observed in the marginal rocks. †Their
506 proximity to the granitic footwall may account for some or all of the variation observed, however,
507 some enrichment may also be attributed to trapped liquid (estimated following Maier and Barnes,
508 1999; McDonald et al., 2009). Regardless of within-sample variation, a small but systematic
509 increase of REE contents can be observed from the troctolites at the base of the succession to the
510 gabbroic units at the top.

511 4.2.3 PGE and Au

512 For this study 28 samples from a range of lithologies have beenwere selected for fire assay; and the
513 results, normalized to chondrite values (Lodders, 2003), are plotted in Fig. 11. Results for †total
514 PGE range from 12 to 12,300 ppb with additional 1.1 to 1100 ppb Au.

515 Upper Zone and TGA Sequence gabbroic rocks display flat profiles across the IPGE and after a
516 moderate increase of concentration also a flat profile across the PPGE and Au. Samples of the
517 troctolites are mostly characterized by mildly sloping IPGE and except for a mineralized sample
518 byhave flat PPGE distributions. The Sserpentinized harzburgiteie lithologies exhibits strongly
519 fractionatedion but within this group identical pattern with Pd/Ir of 177. The rocks are enriched
520 in Pd relative to Pt withand Au beingis depleted relative to Pd. This pattern is also seen for
521 theidentical for that of the mineralized troctolite sample. A sample of the basal pyroxenite is
522 characterized by unfractionated PGE (Fig. 11).

523 Fig. 11 displays variation diagrams of S versus Cu, Pt and Pt. It can be seen that Cu and S exhibit
524 an excellent correlation, whereas the correlation of S and Pt/ or Pd is significantly weakerpoorer.
525 Sulfur levels are overall very low with a maximum of c. 12000 ppm. These levels and correlations
526 are identical to commercial assays in the PTM database (see below)provided courtesy of Platinum
527 Group Metals.

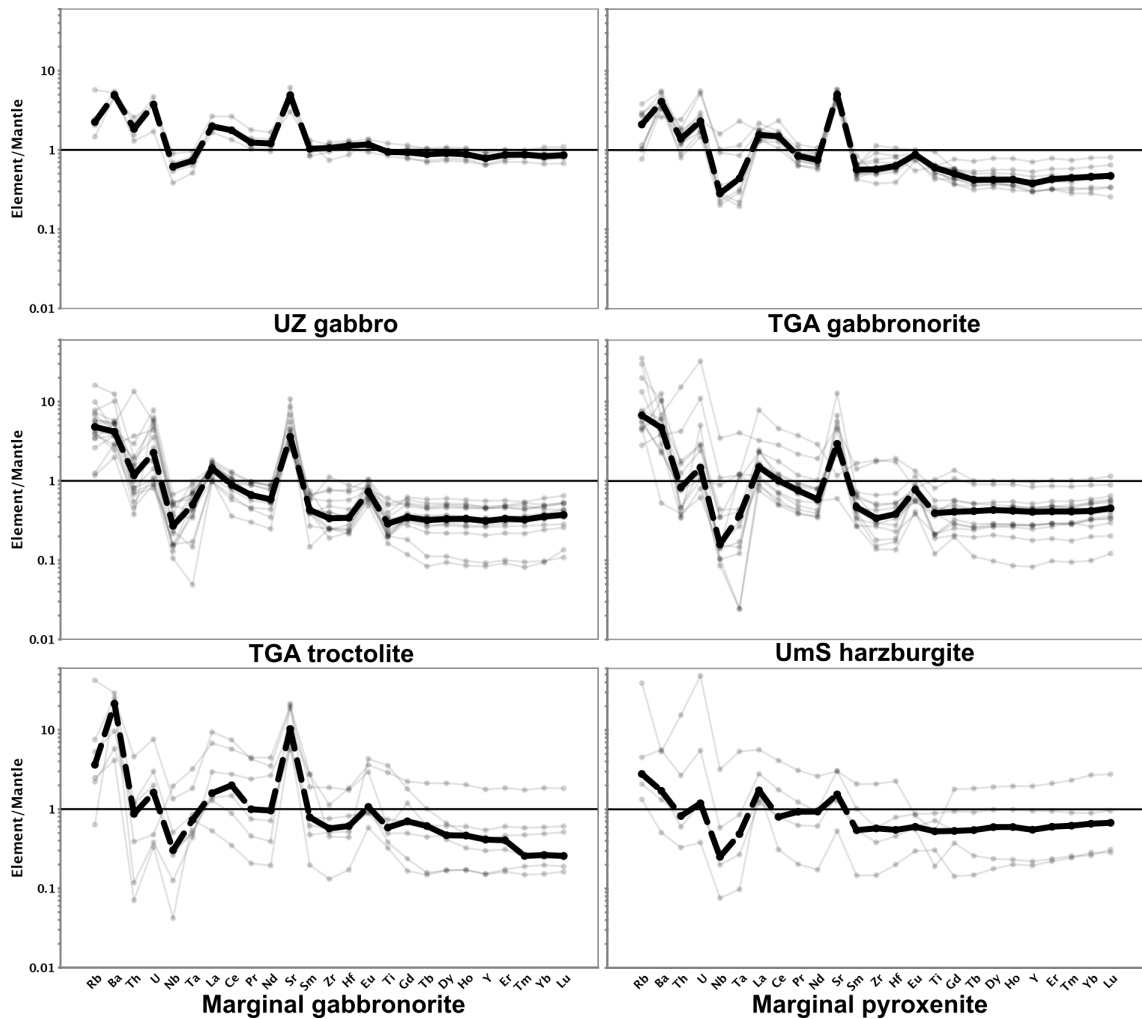


Figure 9: Primitive mantle normalized (Sun and McDonough, 1989) multi-element plots for all six groups of rocks with thick lines showing the average for each group of samples. It can be seen that except for a stratigraphic increase in absolute concentrations the patterns are almost identical. Variations in marginal gabbronorites and pyroxenites are believed to result from contamination by assimilation.

528 **4.2.4 ~~Company assay data~~PGE and Cr assay data provided by Platinum Group**
 529 **Metals**

530 Assay data provided by PTM can be used to assess validity of the results that were presented
 531 above. The available assay data for >100 drill holes from the study area was extracted and ~~are~~
 532 shown in the diagrams below.

533 Figures 12A-C show binary variation diagrams of S vs Cu, Pt and Pd. It can be seen, that Cu
 534 and S show excellent correlation whereas there is only a weak correlation of S ~~with~~, Pt and Pd,
 535 respectively. Pt and Pd ~~have~~exhibit a good correlation ~~among themselves~~ (Table 2). Figure 12D
 536 shows a ternary plot of Pt, Pd and Au. It can be seen, that the majority of assays are dominated
 537 by Pd with Pd/Pt approx. 0.6 and only ~~limited~~low Au ~~content~~. This is in contrast to Pt/Pd
 538 observed in the Merensky Reef and closer to the Pt/Pd observed in some sectors of the Platreef
 539 (Kinnaird, 2005). Low Au is typical ~~for all~~ of the F Zone, whereas ~~in~~ the T Zone and the Aurora
 540 Project Au makes up approximately 20% of the precious metals ~~have approx. 20% Au in the~~
 541 ~~metal~~ budget. Fig. 12D highlights that the anti-correlation of Cr and PGE also applies for the

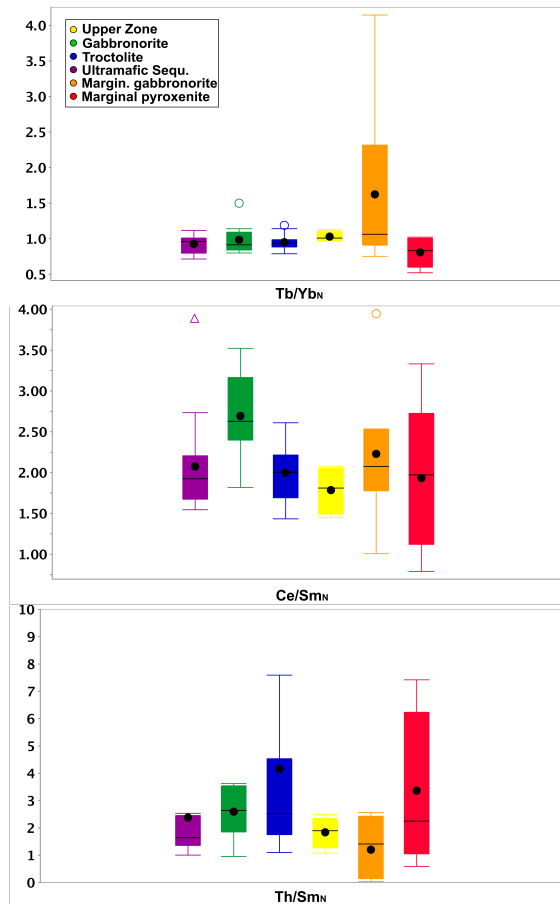


Figure 10: Box plots displaying Tb/Yb_N , Ce/Sm_N and Th/Sm_N values for groups of samples. Color scheme as in Fig. 7. Most variation is exhibited by marginal gabbronorites and pyroxenites, which is interpreted to represent contamination by assimilation. The box represents the inter quartile range with the median represented as horizontal line and the mean as a black circle.

542 rest of the assays in the area. It can be seen that a large number of samples plot in between the
 543 low-PGE/high-Cr and high-Cr/low-PGE trends. This is due to Cr-rich orthopyroxene autoliths
 544 and mingled orthopyroxenitic lithologies that can not be avoided during sampling. This data also
 545 experiences a sampling bias towards mineralized samples (the purpose of the company's sampling
 546 program) and Cr-rich, unmineralized samples are therefore not well-represented.

547 4.3 Lateral variation in lithology and mineralization

548 Typical cross and long sections through the study area (Fig. 3) are shown in Fig. 13 and Fig. 14.
 549 Both sections show the dominant lithology and PTM's assay values for 3E (Pt+Pd+Au) and Cr
 550 as well as Pt/Pd and Cu/Pd.

551 Fig. 13 shows a typical sequence of gabbronorite dominated upper TGA Sequence overlying olivine-
 552 bearing rocks. The base of the TGA Sequence is characterized by heterogeneous and patchy
 553 gabbronorite, norite and troctolite and textures observed in core range from incompletely blended
 554 olivine- or pyroxene-dominant patches to discrete autoliths and xenoliths (Fig. 4A, B). Downwards
 555 this zone grades into "salt and pepper" textured leuco- to melatroctolite.

556 Below the troctolite, strongly altered harzburgite hosts the bulk of the mineralization. Orthopyrox-
 557 enite autoliths occur throughout this part of the succession and where abundant are schematically

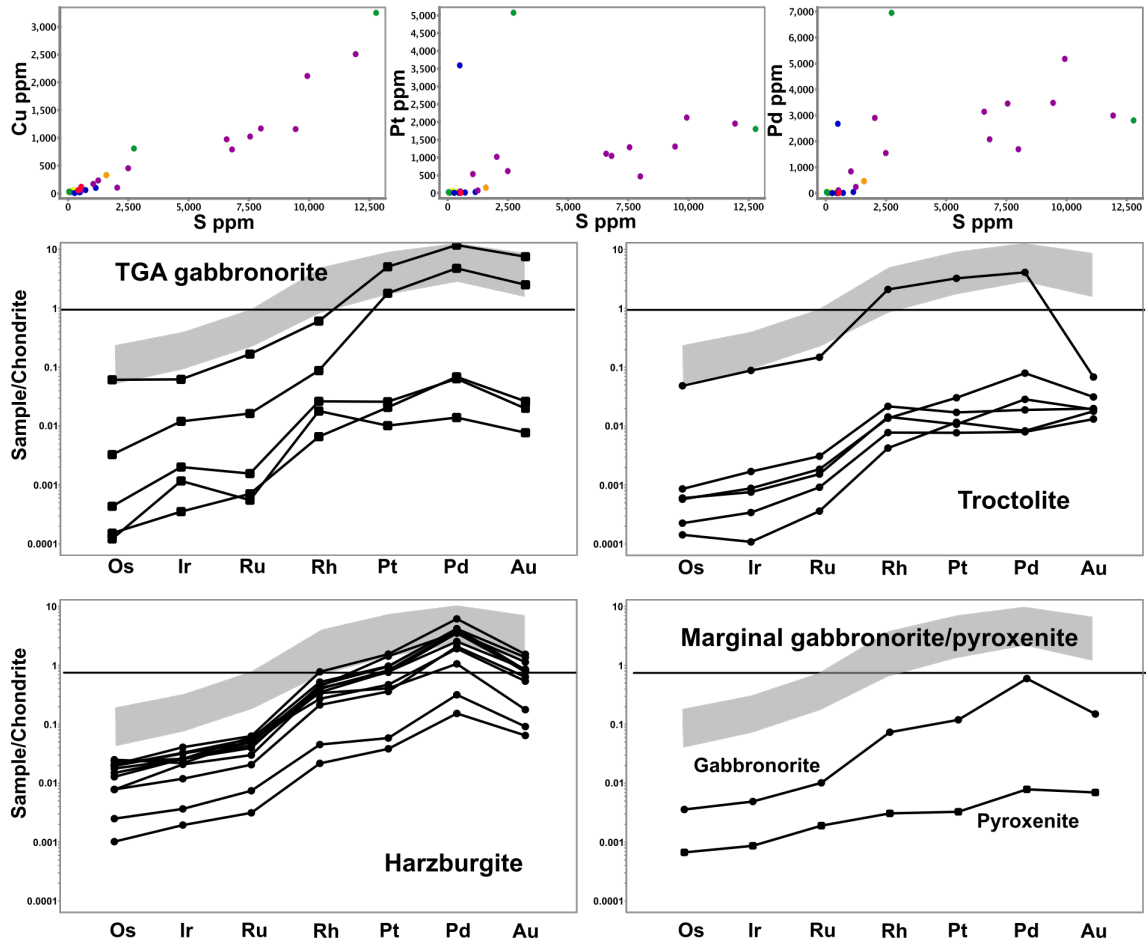


Figure 11: Top: Binary variation diagrams of S vs Cu, Pt and Pd. S vs Cu show an excellent correlation, however the correlation between S and Pt and Pd is weak; Bottom: Chondrite normalized PGE plots for the samples analyzed in this study. Light grey represents PGE distribution from the Turfspruit and Sandsloot high-grade reef-style mineralization in the Northern Lobe (from [Yudovskaya et al., submitted](#) Yudovskaya et al., 2017).

558 indicated in the section. These rocks are typically enriched in Cr and their abundance corre-
 559 relates with the Cr concentration. Below the harzburgites may be more orthopyroxenite, basal
 560 gabbronorites or more troctolites toward the eastern side of the section (drill hole WB091). The
 561 sequence of rocks continues up dip until on the eastern side (not shown) the harzburgites are
 562 directly overlain by sedimentary rocks. In zones of mineralization, the Pt/Pd ratio is fairly con-
 563 stant around 0.6 with a Cu/Pd ratio at approximately 530. As shown above, the mineralization is
 564 dominated by Pd with little Au in the metal budget.

565 The four holes in the long-section (Fig. 14) are located at the western edge of PTMs drilling
 566 in this sector (Fig. 3) and mineralization is hosted by strongly altered, ultramafic rocks of varying
 567 mineralogy and texture. Holes WB163 and WB049 are located at or around the center of the
 568 mineralized zone, while holes WB165 and WB019 are located at its northern and southern edge,
 569 respectively. It can be seen that all four holes share a very similar stratigraphy with Cr-enriched
 570 intervals that appear to correlate between the holes. Mineralization (shown as Pt+Pd+Au) is most
 571 strongly developed in the central section and is poorly developed or absent at the northern and
 572 southern sections. The long section shows well-developed troctolite regardless of the thickness and
 573 3E grade of the harzburgite. This suggests that the intrusion of both suites of rocks is independent
 574 of each other. Pt/Pd and Cu/Pd are again fairly consistent in the mineralized segments.

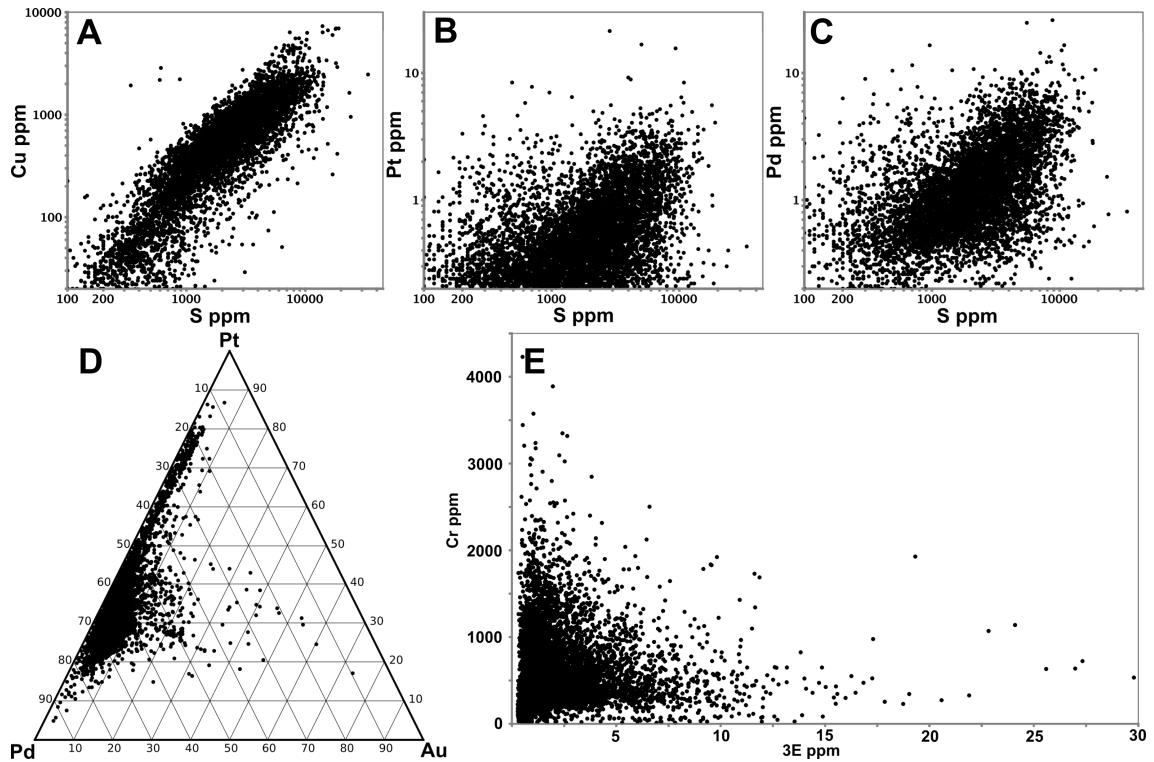


Figure 12: A-C) Binary variation diagrams of chalcophile elements vs sulfur. There is an excellent correlation between Cu and S and a very weak correlation between S and Pt/Pd. D) Ternary diagram showing the relative proportions of Pt, Pd and Au for the assays for the project area. E) Pt+Pd+Au vs Cr diagram highlighting the anti-correlation of precious metals and Cr-rich lithologies. Data filtered for Pt and Pd >0.1 ppm, c. 9500 assays. Sulfide-bearing zones were preferentially sampled by PTM geologists.

575 In summary, the sections show an SW to NE-oriented, tube-shaped and slightly flattened, miner-
 576 alized zone of up to 80 m thickness that is **dominantly** confined to ultramafic rocks. Although
 577 most mineralization is confined to harzburgite and feldspathic pyroxenite, in detail the UmS is a
 578 highly heterogeneous zone with signs of magma mingling, mixing, fluid flow and sulfide remobi-
 579 lization. Grade **idrops** off towards the northern and southern edges before increasing in the next
 580 high-grade, high-thickness harzburgitic zone (not shown in the sections). **Grade is also lower in**
 581 **areas of abundant orthopyroxenite and an anti-correlation of Cr and 3E can be seen.**

582 To visualize this area of the Waterberg Project, a Leapfrog 3D model using the logging data from
 583 >100 drill holes has been created. Due to the nature of company drill logs, some assumptions
 584 and generalizations of logging codes had to be made. This includes grouping various logged rocks
 585 into broader categories, but also the assumption that all logged serpentinite is secondary and the
 586 product of harzburgite alteration. Additionally, given the nature of the ultramafic rocks, the model
 587 uses a >1 g/t 3E grade shell rather than lithology to demonstrate the approximate outline of the
 588 UmS. Figure 15A shows the granite-gneiss basement and the up to 80 m thick grade shell. It
 589 follows what appears to be a basement depression in a northeasterly direction. To its north, a
 590 less-well developed area of PGE mineralization follows the same trend.

591 These depressions may represent a primary feature controlling magma flow, or alternatively, rep-
 592 resent zones of highest heat- and fluid flux and the associated thermal-mechanical erosion. Among
 593 researchers associated with this project the tubular intrusions are referred to as chonoliths (e.g
 594 **Kinnaired et al., 2017**). It is important to stress, that this grade shell was not developed by Plat-

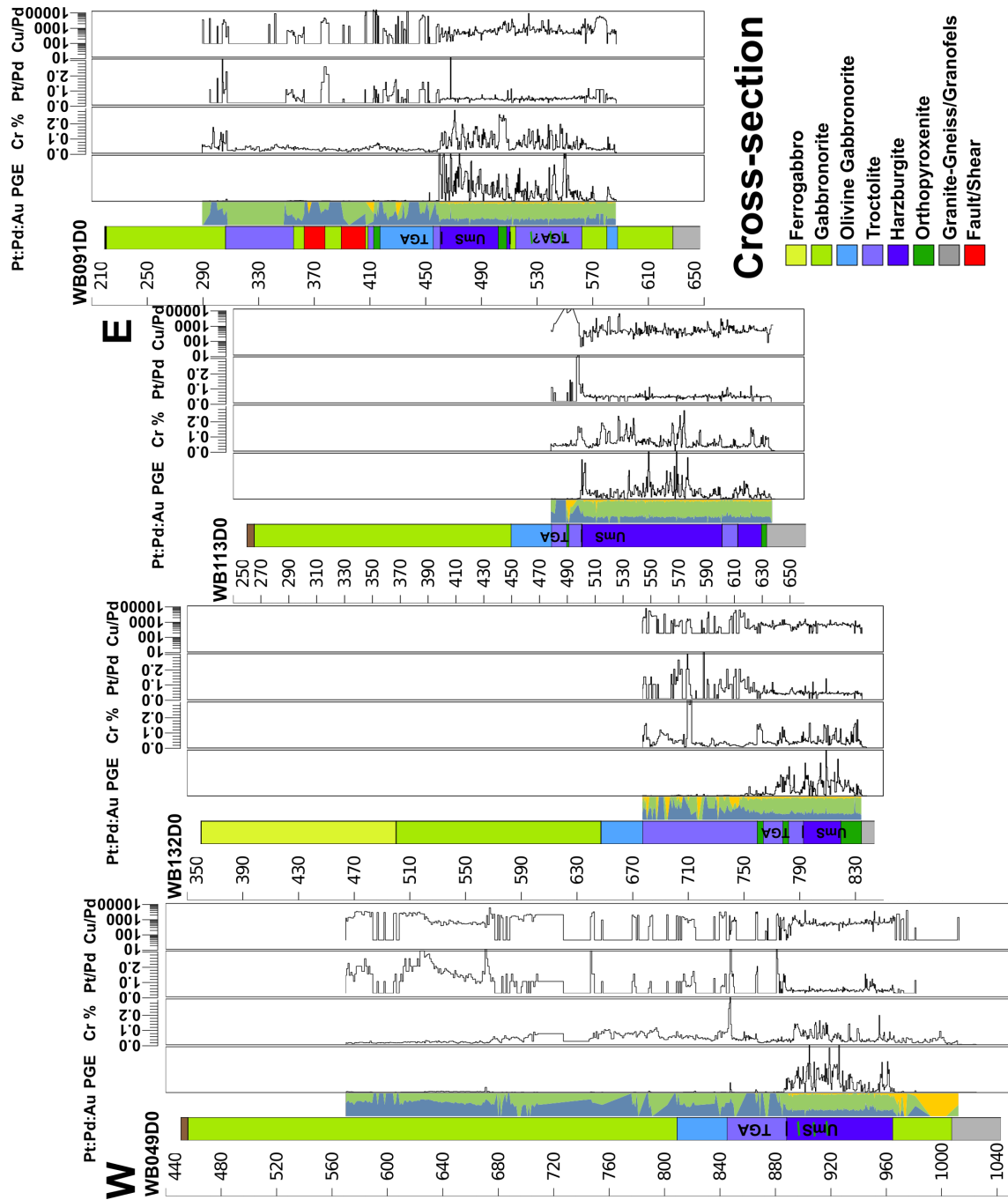


Figure 13: Cross section through the study area as shown in Fig. 3. Columns presented show dominant lithology, the grade of Pt+Pd+Au (no scale), Cr%, Pt/Pd and Cu/Pd extracted from PTM's database. PGE units have been omitted.

595 inum Group Metals to indicate resources and resources but rather models our understanding of
 596 PGE distribution. In Fig. 15B the olivine-bearing lithologies of the lower TGA and Ultramafic
 597 Sequence have been added, and the erosional unconformity of the Waterberg Group sediments and
 598 dolerite sills are shown. The vertical offset in the dolerite dikes may indicate some fault control.
 599 The open area between the upper contact of the olivine-bearing rocks and the base of the sediments
 600 is occupied by gabbroic rocks of the TGA Sequence.

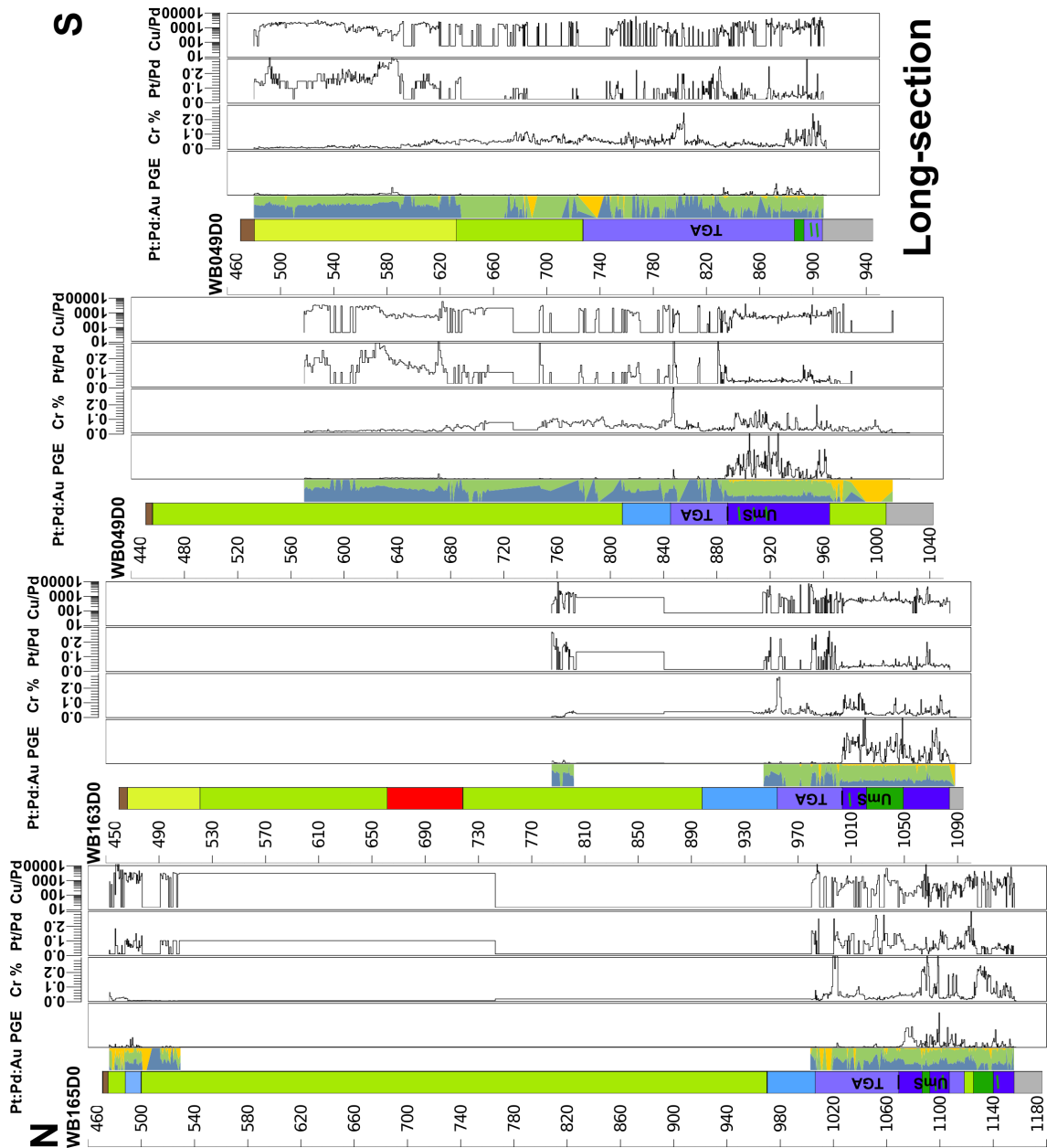


Figure 14: Long section through the study area as shown in Fig. 3. Color scheme as in Fig. 13. Columns presented show dominant lithology, the grade of Pt+Pd+Au (no scale), Cr%, Pt/Pd and Cu/Pd extracted from PTM's database. In contrast to the previous section, harzburgite thickness and associated PGE grade decreases towards the N and S. PGE units have been omitted.

5 Discussion

5.1 Discussion of the data presented

The Northern Lobe of the Bushveld Complex includes the world-class Platreef PGE mineralization and its stratigraphy and mineralization has been the topic of many studies in recent years (e.g. Kinnaird et al., 2005; Kinnaird, 2005; Maier et al., 2008; McDonald and Holwell, 2011; Yudovskaya et al., 2011; Roelofse and Ashwal, 2012; Mitchell and Scoon, 2012; Holwell et al., 2013; Tanner et al., 2014; McDonald et al., 2017; Yudovskaya et al., 2017); also see Yudovskaya et al., subm.).

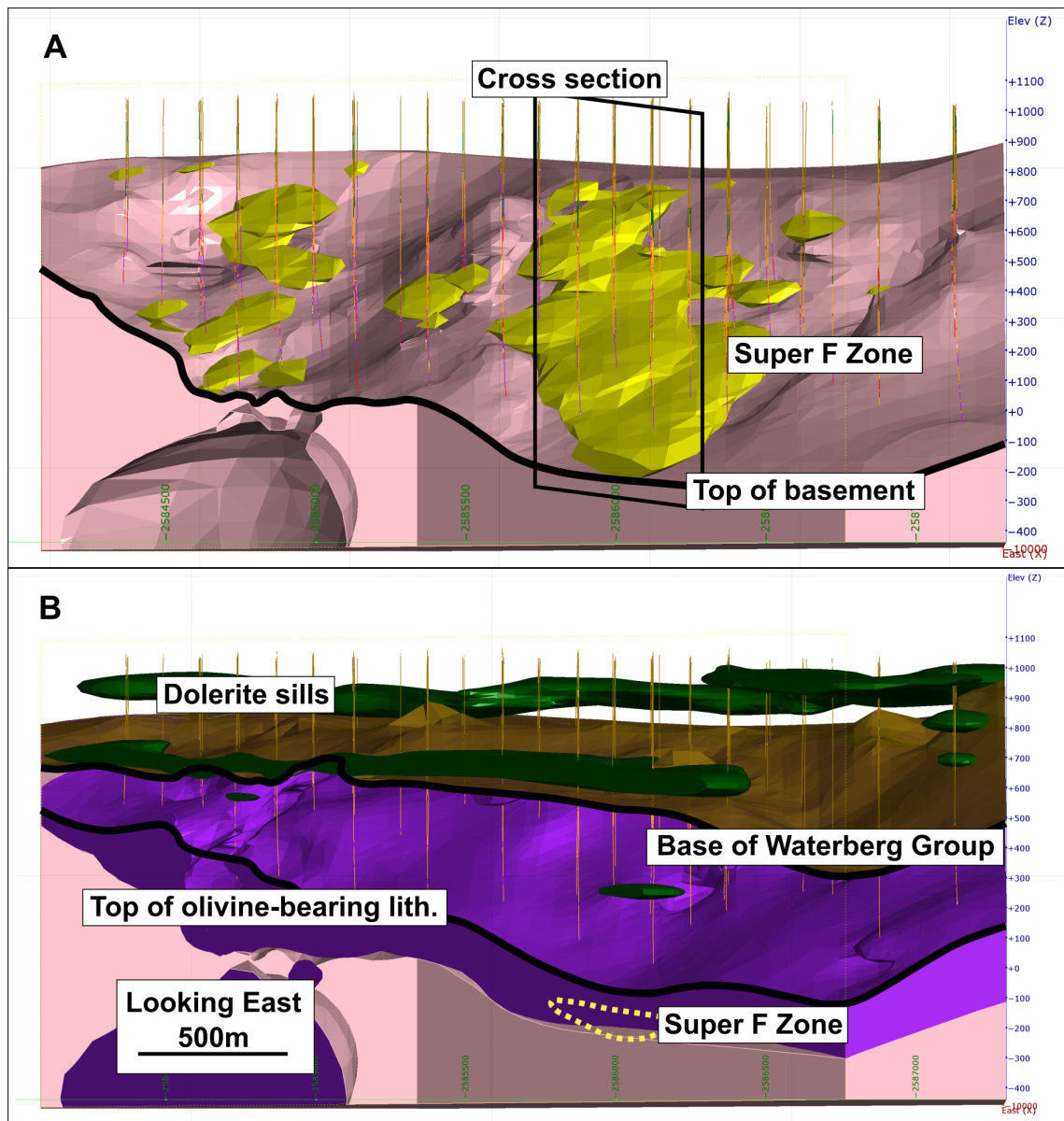


Figure 15: Simplified 3D model of the project area. A) Shown is the geometry of the basement and in yellow a >1 g/t 3E (Pt+Pd+Au) grade shell. The mineralization envelope has a chonolith-shape and is trending in a NE direction. Also shown is the position of holes studied (Fig. 13). B) This panel shows the distribution of the olivine-bearing rocks of the Ultramafic and lower TGA Sequence as logged in PTM’s database. The erosional unconformity bringing Waterberg Group sediment in contact with mafic rocks and the dolerite sills are also shown. Note the vertical offset between the two dolerite sheets, perhaps indicating fault control.

608 In particular ~~T~~he correlation of the Platreef and the Northern Lobe’s northernmost, mineral-
 609 ized lithologies at Aurora ~~in-particular~~ has recently received some attention (Harmer et al., 2004;
 610 Manyeruke, 2007; Maier et al., 2008; McDonald and Harmer, 2010; McDonald et al., 2017). Mc-
 611 Donald et al. (2017) describe several key factors that make it unlikely that the Aurora Project is a
 612 simple strike extension of the Platreef and instead suggest, that it represents a “marginal facies” of
 613 the Main Zone above the Troctolite Marker (which is located 1100 m above the base of the Main
 614 Zone). Considering the location of the Waterberg succession less than 20 km north of the Aurora
 615 Project, it is appealing to simply link the two zones as a northern magmatic basin. Some of the
 616 similarities between the upper Main Zone-hosted Aurora mineralization and the Waterberg T Zone

617 are provided by McDonald et al. (2017) and this contribution will expand on ~~comments made in~~
618 ~~their work. As previously mentioned, this contribution has focussed on an area of the Waterberg~~
619 ~~Succession with little to no development~~ development of the upper mineralized sequence (the T
620 ~~Zone). Nevertheless, both mineralized zones and the whole of the stratigraphy will be considered~~
621 ~~when discussing possible correlations with the Northern Lobe.~~

622 In an initial study, laser-ablation U/Pb dating by Huthmann et al. (2016) demonstrated that zircons
623 from mafic rocks of the succession have an age that is within error identical to ages published for the
624 Bushveld Complex. This study also showed, that the sedimentary rocks unconformably overlying
625 the coarse-grained mafic to ultramafic rocks have a maximum depositional age of 2045 Ma with
626 what is interpreted to be an ash-rich paleosol in-between (Yudovskaya et al., 2015). Given the
627 absence of more evolved mafic rocks, i.e. apatite-bearing UZ or similar, and the absence of any sort
628 of felsic roof rocks, then several kilometers of material must have been removed between c. 2056 and
629 2045 Ma. The Waterberg Project is characterized by significant erosion, a unique stratigraphy of
630 harzburgites and troctolites, a relatively small size and limited thickness and a position wedged in
631 between the Palala Shear Zone in the North and the Hout River Shear Zone in the South (Fig. 1).
632 This places the succession in a unique situation compared to the rest of the Bushveld Complex. The
633 structural position in particular may have created transtensional spaces and crustal anisotropies
634 along which initial magmas could ascend (Lightfoot and Evans-Lamswood, 2015). Further fault
635 movement until 1.97 Ga brought the succession closer to surface and to a mineable depth (Schaller
636 et al., 1999).

637 As shown by logging and geochemical data, the samples all represent ultramafic to gabbroic cumu-
638 late rocks dominated by varying proportions of olivine, plagioclase, ~~and~~ clino- and orthopyroxene.
639 ~~with~~ Clinopyroxene ~~becoming~~ becomes more important the dominant pyroxene towards the top of
640 the succession. Pigeonite may be found towards the top of the succession, however its appearance
641 is erratic. The lower part of the succession comprises strongly altered harzburgites and feldspathic
642 pyroxenites hosting the F Zone mineralization and is overlain by troctolites. Contrary ~~what has~~
643 ~~been described~~ ~~to~~ at the nearby Aurora prospect (McDonald et al., 2017), no significant carbonate
644 xenoliths or carbonate alteration has been found in the Waterberg Succession.

645 The troctolites are different from what is published on the olivine-bearing gabbroic rocks in the
646 Northern Lobe (the Troctolite Marker, van der Merwe, 1976) and comprise only cumulus plagioclase
647 and olivine. The sharp lower contact and the gradational contact with the overlying gabbroic
648 rocks has been shown in drill core (Fig. 4). The Waterberg troctolites are interpreted to be
649 the result of magma mingling and mixing, and are part of a fractionating sequence eroding the
650 earlier harzburgites. Consequently, based on available data, they are not believed to be the direct
651 lateral equivalent of the Troctolite Marker in the Northern Lobe, which itself is interpreted to
652 be an influx of primitive magma into a pre-existing Main Zone (Tanner et al., 2014). The PGE-
653 undepleted Troctolite Marker and the cryptic pyroxenite intrusions described by these workers
654 ~~however~~ highlight the significant lateral and vertical variations in the Northern Lobe. Furthermore,
655 although the work of Ashwal et al. (2005) and Roelofse and Ashwal (2012) provides a detailed
656 stratigraphy for most of the Northern Lobe, about 490 m of stratigraphy are unaccounted for.
657 Most crucially, the missing segment is at the base of the troctolite marker where ultramafic rocks
658 might be expected.

659 Above the olivine-bearing rocks is a package of noritic to gabbro-noritic rocks, grading into magnetite-
660 bearing gabbros/gabbro-norites. The gabbroic rocks are typically taken to be the equivalent of the
661 Northern Lobe's Main and Upper Zone given their mineralogy. While this may be the case, gabbroic

662 rocks are typical ~~for~~ evolving layered mafic intrusions and their occurrence does not necessitate
663 a connection of magma conduits between the Northern Lobe and the Waterberg Succession

664 ~~and the occurrence of plagioclase, ortho- and clinopyroxene does not necessitate a connection of~~
665 ~~magma chambers. The same does apply to magnetite-bearing rocks.~~

666 The lower part of the succession hosts what are interpreted to be autoliths of Cr-enriched, olivine-
667 bearing orthopyroxenites (which are therefore older). The exact lateral distribution of these rocks
668 is currently ~~insufficiently~~ poorly understood, and some may represent either rafts or perhaps simul-
669 taneously intruded sills. Where these rocks have been assimilated by younger intrusive phases, the
670 resulting drill core sections are characterized by increased Cr levels (Figs. 13 and 14). Additionally,
671 given their unmineralized nature, a commensurate drop in PGE levels can be observed in the assay
672 intervals including these autoliths (Fig. 13 and 14).

673 Highest PGE grade intervals are often found in zones of intense alteration of primary silicates
674 and may contain sulfide stringers and veins. Both features suggest some remobilization of initial
675 sulfides, also leading to a decoupling of sulfides and to a more limited degree of Pt and Pd. This
676 process can be observed in the company assay data presented earlier, where Pd is remobilized
677 preferentially over Pt (Barnes and Liu, 2012). Whether this process has an effect on the overall
678 Pt/Pd ratio is currently undetermined.

679 Major element whole-rock geochemistry places the rocks in three distinct groups, representing the
680 Cr-enriched ~~Marginal~~ basal orthopyroxenites, the harzburgites of the Ultramafic Sequence, and
681 the Troctolite-Gabbro-norite-Anorthosite Sequence and Upper Zone. Rocks of the TGA Sequence
682 form a continuous trend from high-Mg, olivine-rich troctolites to the magnetite-bearing gabbroic
683 rocks ~~higher up in the sequence~~ of the Upper Zone. This trend may indicate that the TGA Se-
684 quence and the Upper Zone of the Waterberg Succession form a continuum and should be grouped
685 together. The marginal gabbroic rocks resemble the TGA rocks in chemistry and mineralogy,
686 and ~~are thought to be related to~~ may represent downward injections into older units ~~earlier phases~~.
687 Outliers in troctolite composition may be related to variable amounts of oikocrystic orthopyroxene
688 and contamination by the underlying harzburgite and orthopyroxenite. Trends of harzburgites
689 and troctolites differ, suggesting the crystallization of harzburgite from a more Mg-rich liquid and
690 consequently the crystallization of more Mg-rich olivine.

691 Normalized REE pattern show near uniformity (e.g. fairly consistent Ce/Yb, Th/Nd) with a minor
692 stratigraphic increase in abundances. Except for Eu, all REE are incompatible in the cumulus
693 phases of the Waterberg succession (olivine, orthopyroxene, plagioclase, clinopyroxene) which is
694 reflected in the primitive mantle-normalized diagrams. Accessory phases (other than zircon) that
695 would concentrate LREE have not been observed and hence the REE budget is controlled by
696 intercumulus liquid (Maier and Barnes, 1998). Normalized REE values below one are interpreted
697 to reflect the fact that the rocks of the Waterberg Succession are crystal cumulates. ~~and that t~~The
698 incompatible element budget of the parental magma was either retained in a staging chamber or
699 lost with migrating interstitial liquid. The variation in incompatible elements and REE contents
700 and the associated extreme outliers, particularly in the basal rocks, are interpreted to represent wall
701 rock contamination. Gabbroic rocks are characterized by $Rb_N < Ba_N$, while the opposite is true for
702 ultramafic rocks. Troctolite Rb/Ba_N are approx. 1, again suggesting contamination of troctolite
703 by underlying harzburgites. Estimates of trapped liquids using La or Zr (not shown; Maier and
704 Barnes, 1999; McDonald et al., 2009) exhibit a good correlation with peaks in incompatible element
705 abundances, ~~however.~~ Given the interaction of pyroxenites and granite-gneisses observed in drill
706 core, the validity of these calculations, however, is questionable for the Waterberg Succession.

707 The slight upward stratigraphic increase in LREE observed is interpreted to be related to the
708 increased proportions of clinopyroxene in the rocks. Troughs for the elements Th, Rb, Nb, and
709 Ta are fairly typical for Bushveld rocks and generally interpreted to represent contamination by
710 lower-mid continental crust (Barnes and Maier, 2002).

711

712 5.2 Correlation with the Aurora Project ~~the Northern Lobe~~

713 McDonald et al. (2017) recently presented data demonstrating strong similarities between the
714 Aurora Project and parts of the Waterberg Succession. The data presented in their work may be
715 used to create a “simplified” and continuous emplacement model. At this point, most areas of the
716 Northern Lobe are however not nearly as well-researched as the well-exposed open cut mines at
717 Sandsloot. Caution and reliance on published data is therefore needed when correlating individual
718 prospects.

719 Both the Platreef and the Waterberg Succession exhibit variations in rock type and mineralization
720 along their strike, although compared to the Platreef the Waterberg Succession is small with
721 approximately 15 km strike length. Dynamic emplacement environments with multiple, channelized
722 magma injections along a dip westerly to northwesterly direction (rather than a north to south
723 magma flow) have been proposed for the Platreef (Yudovskaya et al., 2017; cf. Barnes et al.,
724 2016), and may together with floor rock control (Kinnaird et al., 2005) be used to explain clear
725 differences along strike. The existing similarities between individual sectors (such as Aurora and
726 the Waterberg Project) may be attributed to the fact, that all of them are related to the Bushveld
727 Large Igneous Province and hence share the same melting event.

728 McDonald et al. (2017) describe the Aurora Project as consisting of three main units, namely Unit
729 1 with peridotites and melagabbonorites, Unit 2 with gabbonorites and leucogabbonorites and
730 Unit 3 comprising pigeonite gabbonorites. Additionally, Aurora comprises zones of sometimes
731 pegmatitic magnetite gabbros and olivine-bearing gabbroic rocks. Mineralization is hosted pre-
732 dominantly by felsic rocks. The mineralogical details and geochemical data provided in their work
733 suggests the following correlation:

734 Unit 1 at Aurora is characterized by orthopyroxenite, enrichment in Cr and consequently high
735 Cr/MgO ratios. These features suggest that Unit 1 might correlate to the Cr-rich marginal or-
736 thopyroxenites described for the Waterberg Succession. This interpretation is supported by min-
737 eralogy and similar trends and positions on bivariate major and trace element plots and close to
738 identical trace element ratios.

739 Both Unit 2 and 3 at Aurora are more evolved gabbroic rocks interpreted to correlate with the
740 upper TGA Sequence of the Waterberg Succession. This interpretation is again supported by
741 both mineralogical and geochemical features. Where developed, the upper TGA Sequence in
742 the Waterberg Succession hosts two mineralized zones, often with a middling in between. It
743 features olivine-bearing rocks, the appearance of pegmatites and pigeonite. This is comparable
744 to the variable nature of rocks in the Aurora Project, also characterized by several mineralized
745 zones. Geochemically, available data for the upper TGA Sequence again shares similar positions
746 on bivariate plots and almost identical trace element ratios with the Aurora Project.

747 The main geochemical difference between the two deposits exists in Rb/Ba_N ratios, with gener-
748 ally lower values for Aurora. McDonald et al. (2017) report a carbonate overprint and carbonate

749 assimilation for the Aurora project, ~~while n~~ No significant carbonate has been found at the Water-
750 berg, indicating purely granite-gneiss host rocks. The differing Rb/Ba_N ratios ~~are may~~ therefore
751 ~~interpreted to~~ be the result of different host rocks.

752 In terms of previous metals, the Aurora Project is characterized by approximately 20% Au in its
753 precious metals budget (Fig. 16). This also holds true for the T Zone of the Waterberg Project.
754 It is worth noting, however, that elevated Au/PGE ratios have not only been recorded at Aurora,
755 the T Zone and Moorddrift (Harmer et al., 2004; Maier et al., 2008; McDonald and Harmer, 2010;
756 Maier and Barnes, 2010; Holwell et al., 2013; McDonald et al., 2017), but also for the Upper Reef
757 at Turfspruit (Yudovskaya et al., 2017), and the Bastard Reef (albeit at very low levels, Maier and
758 Barnes, 2008). Hence, elevated Au may be a feature associated with higher stratigraphic position
759 in the mafic sequence, given no previous metal depletion. Considering the weak grade at Aurora
760 compared to the Waterberg Project, the prospect might represent a southern extension of the
761 Waterberg Succession rather than the other way around.

762 This ~~interpreted possible~~ correlation between T Zone mineralization and ~~for~~ the Aurora Project does
763 not account for the economically significant F mineralized Zone, which is located stratigraphically
764 below the T Zone. ~~leaves the economically significant lower section of the succession unaccounted~~
765 ~~for. The F Zone is located stratigraphically below the T Zone and~~ Following the argument of
766 Aurora being located in the upper Main Zone (McDonald et al., 2017), the F Zone ~~may~~ must
767 ~~therefore either~~ represent a highly unusual, richly-mineralized lower Main Zone of olivine-bearing
768 rocks, i.e. the Troctolite Marker, or a marginal, very northern expression of the Critical Zone, i.e.
769 the Platreef. ~~Furthermore, i~~

770 It is crucial to note, that on the farm Harriet's Wish in the far north of the Northern Lobe (Fig.
771 2A) the igneous units exhibit a pronounced change in strike direction from NNW to NNE when
772 crossing the Hout River Shear Zone. The shear zone itself has, as far as the authors are aware,
773 not been intersected in drill core. Despite the mineralogical and geochemical similarities described
774 above, the exact nature of the relationship of Waterberg Succession and ~~Northern Lobe (s.s.)~~ Aurora
775 Project therefore still needs to be established.

776 5.3 Correlation with the Platreef

777 Mineralization in the F Zone of the Waterberg Succession is characterized by its anti-correlation
778 with Cr, a Pt/Pd ratio of 0.6 and approximately 5% Au in the metal budget (Fig. 16). Ni/Cu is
779 significantly higher than other Northern Lobe ~~operations~~ mines at 6-8. Chondrite-normalized PGE
780 patterns show mildly fractionated IPGE and significantly enriched and also mildly fractionated
781 PPGE. ~~This fractionation between IPGE and PPGE possibly reflects the lower temperature melts~~
782 ~~in the Proterozoic (compared to the Archean. Mungall and Brennan, 2014).~~ The PGE have some
783 resemblance to patterns observed at various Platreef projects (Maier et al., 2008 and references
784 therein, ~~Yudovskaya et al., submitted~~ Yudovskaya et al., 2017) and what is typical for ultramafic
785 hosts in the Bushveld Complex (Naldrett et al., 2011), ~~although we observe~~ The slightly higher
786 fractionation ~~observed~~ between IPGE and PPGE ~~that~~ may be related to IPGE (and chromite)
787 retardation ~~together with chromite~~ somewhere at depth. The low Pt/Pd ratios are typical for those
788 recorded for the lower Platreef (e.g. Kinnaird, 2005) while the (Pt+Pd)/Au and Ni/Cu (adjusted
789 for silicate Ni due to harzburgite host) place the F Zone in a field with Platreef exploration and
790 mining projects (Fig. 4 in McDonald et al., 2017). The absence of a correlation between PGE and
791 S is typical for disseminated mineralization at the base of the Platreef (Hutchinson and Kinnaird,
792 2005). The poor correlation between the PGE and S is ascribed to the remobilization and partial

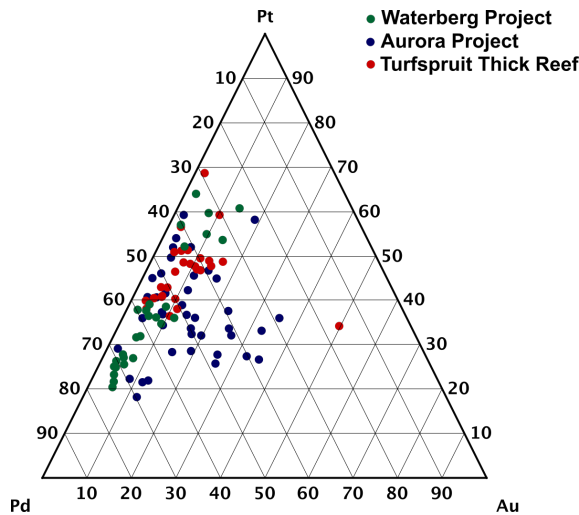


Figure 16: Ternary diagram for Pt, Pd and Au displaying data for the Waterberg Project, the Aurora Project (McDonald et al., 2017) and Turfspruit (Yudovskaya et al., 2017).

793 removal of sulfides after emplacement, thereby selectively remobilizing Pd over Pt. Cr/MgO ratios
 794 are consistently low and dissimilar to the Platreef unit ~~however~~ (McDonald and Holwell, 2011).

795 Analogously to the Platreef, the mineralized harzburgites and feldspathic pyroxenites are inter-
 796 preted to have potentially been emplaced as sill- or chonolith-like bodies. Cross- and-long sections
 797 as well as a 3D representation of one of the Super F Zones have been presented in Figs. 13, 14 and
 798 15, respectively. In these figures, it can be seen that where the these lithologies are absent, their
 799 space it taken up by the otherwise overlying TGA Sequence. This is particularly apparent in Fig.
 800 15, where grade is sparse above the “basement high” in the center of the figure and increases both
 801 to the north and south.

802 The reasons for sulfide saturation are only speculative at present. Possible options may be the
 803 assimilation of potentially Cr-rich orthopyroxenites or mixing of successive melt fluxes. Given the
 804 granite-gneiss basement and the extreme scarcity of xenoliths ~~of what might have been sedimentary~~
 805 ~~reeks~~, sulfide saturation due to sulfur-rich host-rock assimilations appears unlikely and the sulfur
 806 source is under investigation. Detailed petrographic analysis of a wide range of thin sections
 807 confirms ~~athe~~ remobilization of sulfides observed in core and suspected from geochemical data,
 808 and hence the original distribution and mineralogy of the ore minerals is uncertain. Detailed
 809 comparisons of the F Zone with the lower part of the troctolite marker are hampered by the lack
 810 of published and peer-reviewed descriptions and data.

811 A preliminary model

812 In summary, the lower mineralized zone of the Waterberg Project has been shown to have similar-
 813 ities with the Aurora Project and the Platreef, while also displaying clear differences. Any model
 814 for the Waterberg Succession must account for the following observations (Kinnaid et al., 2014;
 815 Huthmann et al., 2016; Kinnaid et al., 2017):

816 ~~While there is still an abundance of research to be completed, any model for the Waterberg~~
 817 ~~Succession must account for all of the following observations (also see Kinnaid et al., 2014; Huthmann et al., 2016;~~
 818 ~~Kinnaid et al., subm.):~~

- 819 • The Waterberg Succession contains a magnetite-bearing gabbroic Upper Zone, a mineralized
820 Troctolite-Gabbronorite-Anorthosite Sequence and a lower, mineralized Ultramafic Sequence
821 of harzburgites and feldspathic pyroxenite.
- 822 • The troctolites of the Waterberg Succession are true plagioclase and olivine cumulates un-
823 conformably overlying ultramafic rocks. They are characterized by a significant thickness,
824 high-Mg and the fractionation into olivine norite and later gabbronorite.
- 825 • The overall thickness of the Waterberg Succession is approximately 25% of the Northern
826 Lobe, however due to an erosional unconformity an unknown amount of material (several
827 km?) as well as roof rocks of unknown nature ~~have as of yet not been intercepted in drill~~
828 ~~core~~ ~~are missing~~.
- 829 • The mineralization of the Waterberg T zone contains c. 20% Au in the metal budget. ~~and b~~
- 830 • Based on mineralogy and chemistry, the Aurora Project may represent the southern margin
831 of the Waterberg Succession.
- 832 • Despite being hosted by harzburgites rather than pyroxenites, the F Zone mineralization
833 shares certain characteristics with the Platreef. It is Pd-dominated and Au-poor, however,
834 Cr/MgO are dissimilar from the Platreef. The Waterberg's F Zone does not form "reefs" and
835 mineralization occurs along high-aspect ratio elongated bodies or chonoliths.
- 836 • Geochemical results presented show Bushveld-type cumulate signatures.

837 Currently many aspects of the development history of the Waterberg Succession are not fully
838 resolved, ~~however~~ ~~and~~ its unique structural position ~~may be one major aspect~~ ~~is an important~~
839 ~~example~~. A simplified model for the evolution of the Waterberg Succession is presented in Fig. 17.
840 The magmatic history of the area is believed to have started with finger-like intrusions of marginal
841 orthopyroxenites intruding into a host rock of granite-gneiss and perhaps overlying sedimentary
842 rocks. Unlike the Northern Lobe, the Waterberg Succession is situated in the Southern Marginal
843 Zone of the Limpopo Belt (van Reenen et al., 1987), wedged in between the Hout River and Palala
844 Shear Zones. Given the tectonic setting of the Limpopo Belt, this initial emplacement may have
845 been facilitated either by pre-existing anisotropies related to faulting or perhaps ongoing faulting
846 during the time of emplacement (Schaller et al., 1999; Clarke et al., 2009; Lightfoot and Evans-
847 Lamswood, 2015). Figure 17 displays the initial stages near a possible basement - cover sequence
848 contact. Whether this is indeed the case is unknown and depth of emplacement may instead be
849 the depth of neutral buoyancy of the ascending liquid magma. Given the age and location of the
850 Waterberg Succession (Huthmann et al., 2016), the liquid magmas are of course ultimately related
851 to the Bushveld Large Igneous Province.

852 With increasing magma flux, ~~these~~ ~~the~~ magma conduits would experience lateral dilation until
853 eventually forming larger elongated bodies lobes. Maximum ~~heat and~~ liquid flux would ~~however~~ be
854 focused on their respective cores, where the crystallization is suppressed due to the high heat flux
855 (Hon et al., 1994). These heated zones of weakness could then be utilized by subsequent intrusion
856 of parental crystal-rich liquids for the harzburgites, in the process widening the conduit while
857 assimilating and transporting earlier rocks (Robertson et al., 2015). The harzburgites are thought
858 to have acted as the transport medium for sulfide droplets, perhaps remobilizing dense sulfide from
859 some initial staging zone (McDonald et al., 2009). Given the tube-like shape of the grade shells
860 and the fairly even distribution of grade throughout the shell, a slumping of sulfides along the
861 basement is not considered viable. ~~Due to recent findings of extremely high partition coefficients~~

862 for PGE (10^5 to 10^6 , Mungall and Brenan, 2014), the kinetics of the interaction between sulfide
863 liquid and magma and the architecture of the emplacement zone may however be the crucial
864 factor (Barnes et al., 2016), rather than large pools of sulfide liquid at depth. The geometry of
865 the emplacement zone in particular may be responsible for the substantial thickness and grade
866 of the ore zones, leading to what Platinum Group Metals refers to as Super F Zones. Mungall
867 and Brenan (2014) recently demonstrated extremely high partition coefficients of 10^5 to 10^6 for
868 PGE. This means, that the kinetics of the interaction between sulfide liquid and magma and the
869 architecture of the emplacement zone may be more important than large pools of sulfide liquid at
870 depth. The geometry of the emplacement zone in particular may be responsible for the substantial
871 thickness and grade of the Super F Zones. ~~The F Zones and the Waterberg Succession overall~~
872 ~~are truly exceptional with an indicated resource of more than 24 million ounces 4E the deposit is~~
873 ~~still open at depth.~~ The position of the mineralized zones and the distribution of sulfides therein
874 again appears to suggest, that the UmS represents zones of crystallization of the respective carrier
875 liquids, and not a basal accumulation of sulfides. Constant Cu/Pd ratios observed in PTMs assay
876 data suggest one common PGE reservoir for this particular Super F Zone. ~~The F Zones and the~~
877 ~~Waterberg Succession overall are truly exceptional and have an indicated resource of more than~~
878 ~~24 million ounces 4E (Pt+Pd+Au+Rh).~~ The deposit is still open at depth.

879 Following the emplacement of mineralized harzburgitic lithologies, ~~the~~ subsequent intrusions
880 ~~would~~ could utilize the extensive pre-heating of country rocks to form a more laterally extensive
881 sheet of troctolites by thermo-mechanical erosion. This was perhaps, ~~perhaps~~ assisted by pre-
882 existing anisotropies along a basement-sedimentary rock interface. At this point, the Waterberg
883 Succession was moving from a stage of finger-like liquid flow and lateral dilation to a stage of sheet-
884 like ~~bodies~~ lobes with sufficient thickness to allow for in-situ fractionation. This ultimately led to the
885 formation of a sequence of troctolites-gabbro-norites-magnetite-bearing gabbros and to a transition
886 from heterogeneous to homogeneous flow. It is envisioned, that the formation of troctolitic units
887 was related to the mixing of gabbroic and peridotitic crystal-rich ~~liquids~~ magmas in the feeder
888 zone of the succession (Renna and Tribuzio, 2011; Saper and Liang, 2014). The subsequent in-
889 situ fractionation of gabbroic magmas may have been disturbed by new cryptic influxes of more
890 gabbroic liquids (cf. Tanner et al., 2014). Fractionation may ~~leading~~ have led to a sequence that
891 ~~may have included now eroded fairly evolved rocks of a gabbroic nature~~ rocks comparable to what
892 can be seen in the upper Upper Zone of the Northern Lobe (Ashwal et al., 2005), however, in the
893 Waterberg Project this zone has been eroded. ~~Mineralized cores at the base of the troctolites were~~
894 ~~preserved and the extensive alteration and sulfide remobilization in the harzburgites may be a sign~~
895 ~~of continuing heat and fluid flux in the system. Occasional pegmatoidal and “vari-textured” rocks~~
896 ~~throughout the succession perhaps attest to this continuing interaction of heat with the footwall.~~
897 Mineralized harzburgite “cores” at the base of the troctolites were preserved, and the extensive
898 alteration and sulfide remobilization in the harzburgites may be a sign of continuing heat and
899 fluid flux in the system. The occasional pegmatoidal and “vari-textured” rocks throughout the
900 succession perhaps attest to this continuing interaction of heat with the footwall.

901 The exact nature of the connection between Waterberg Project and the aforementioned Aurora
902 Project can only be estimated. Taking into account the occurrence of early orthopyroxenites and
903 later gabbroic lithologies, perhaps both areas were connected intermittently with assimilation of
904 dolomite being locally important at Aurora. Correlation of the two projects might indicate that
905 both of them form a northern ~~“basin”~~ partially or intermittently connected magmatic basin. This
906 basin is internally subdivided by the Hout River and other small shear zones and separated from
907 the south by a basement high south of Aurora (Kinnaird et al., 2005).

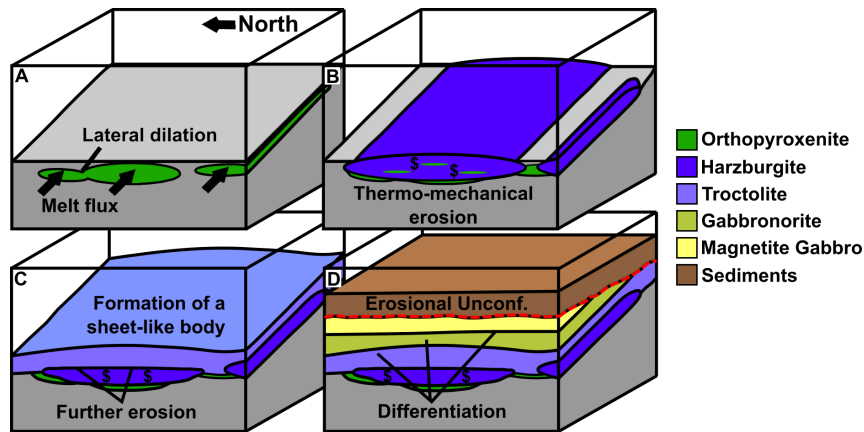


Figure 17: Conceptual model for the emplacement of the lower part (excluding the T Zone mineralization) of the Waterberg Succession. A: Emplacement of marginal orthopyroxenites as finger-like elongated bodies. Lateral dilation with continuing magma flow. B: Emplacement of harzburgitic magma and sulfides by thermo-mechanical erosion of earlier intrusive phases and host rock. C: Emplacement of troctoliteic magma, marking the departure from a finger-like geometry and the formation of sheets. D: After the emplacement and fractionation of more magma, the area experienced extensive uplift and the deposition of Waterberg Group Sediments on an erosional unconformity.

908 As a final step, uplift and later subsidence led to an erosional unconformity and the deposition of
 909 Waterberg Group Sediments on top of the succession. This step is crucial, as without significant
 910 uplift and erosion the succession might have been covered by ~~what can be assumed to be~~ several
 911 kilometers of evolved rocks.

912 The model presented above requires the intrusion of two distinct magmas during the course of the
 913 formation of the Waterberg Succession, one being peridotitic and one gabbroic in character. Given
 914 the similarities of the Ultramafic Sequence with the Platreef, and of the TGA Sequence with the
 915 Main Zone, it is envisioned that the former crystallized from a Critical Zone-type ~~liquid~~ magma
 916 while the latter represents a Main Zone-type ~~liquid~~ magma (or ~~liquids~~ magmas). This is not meant
 917 to imply a direct connection of the Waterberg area with either the main Bushveld or the Northern
 918 Lobe, but rather refers to the fact that all intrusions belong to the same large igneous province.

919 6 Conclusion

920 The Waterberg Succession is a truly outstanding and exciting new PGE discovery, and will ~~change~~
 921 ~~the PGE market~~ with its high grade and thickness ~~change the PGE market~~. It shares ~~common~~ fea-
 922 tures with mining and exploration prospects to the south, while simultaneously exhibiting unique
 923 characteristics. The combination of rock types, type and distribution of mineralization, and tec-
 924 tonic setting is unique and presented here for the first time. Based on observations and geochemical
 925 results, the Waterberg Succession may be linked with the Aurora Project to the south, with both
 926 projects possibly representing a separate basin rather than a marginal extension of the Northern
 927 Lobe. A first conceptual model for the area has been presented and shows how recent advances in
 928 our understanding of partition coefficients, fluid dynamics, and the continued work of colleagues
 929 in other parts of the Bushveld leads to a better understanding of this magmatic system.

930 ~~The conclusion of the Waterberg Project not representing a mere strike extension of the Northern~~
 931 ~~Lobe is excellent news for explorers of the Bushveld Complex and demonstrates that mineralized~~

932 ~~successions can be found along the margins of the complex. Cooperation of industry and academia,~~
933 ~~aided by 21st century geophysical techniques may be used to re-evaluate areas previously thought~~
934 ~~to be barren.~~The conclusion that the Waterberg Succession does not represent a simple strike
935 extension of the Northern Lobe is excellent news for explorers of the Bushveld Complex. It demon-
936 strates, that cooperation of industry and academia, aided by 21st century geophysical techniques,
937 can lead to significant discoveries in well-explored terrains. Rather than obstructing deposit for-
938 mation, structural features and sedimentary sequences may aid by concentrating melt flow and
939 facilitating later uplift.

940 Acknowledgements

941 We would like to acknowledge the support and funding received from Platinum Group Metals. We
942 would also like to acknowledge CIMERA. The work at IGEM RAS was supported by the Russian
943 Foundation for Basic Research (grants 14-05-00448 and 17-05-00456). [The manuscript greatly](#)
944 [benefited from the detailed comments by P. Lightfoot and W. Maier.](#)

945 References

- 946 Ashwal, L. D., Webb, S. J., Knoper, M. W., 2005. Magmatic stratigraphy in the Bushveld Northern
947 Lobe: continuous geophysical and mineralogical data from the 2950 m Bellevue drillcore. South
948 African Journal of Geology 108 (2), 199–232.
- 949 Barnes, S. J., Cruden, A. R., Arndt, N., Saumur, B. M., 2016. The mineral system approach
950 applied to magmatic Ni–Cu–PGE sulphide deposits. Ore Geology Reviews 76 (C), 296–316.
- 951 Barnes, S. J., Liu, W., Feb. 2012. Pt and Pd mobility in hydrothermal fluids: Evidence from
952 komatiites and from thermodynamic modelling. Ore Geology Reviews 44 (C), 49–58.
- 953 Barnes, S.-J., Maier, W. D., 2002. Platinum-Group Element Distributions in the Rustenburg Lay-
954 ered Suite of the Bushveld Complex, South Africa. In: Cabri, L. J. (Ed.), The Geology, Geochem-
955 istry, Mineralogy and Mineral Beneficiation of Platinum-Group Elements. Canadian Institute of
956 Mining, Metallurgy and Petroleum Special Volume 54, pp. 431–458.
- 957 Barton, J. M., Klemd, R., Zeh, A., 2006. The Limpopo belt: A result of Archean to Proterozoic,
958 Turkic-type orogenesis? Geological Society of America Special Paper 405, 315–332.
- 959 Buick, I. S., Maas, R., Gibson, R. L., 2001. Precise U–Pb titanite age constraints on the em-
960 placement of the Bushveld Complex, South Africa. Journal of the Geological Society 158 (1),
961 3–6.
- 962 Callaghan, C. C., Eriksson, P. G., Snyman, C. P., 1991. The sedimentology of the Waterberg Group
963 in the Transvaal, South Africa: An overview. Journal of African Earth Sciences 13 (1), 121–139.
- 964 Cawthorn, R. G., Webb, S. J., 2001. Connectivity between the western and eastern limbs of the
965 Bushveld Complex. Tectonophysics 330 (3-4), 195–209.
- 966 Clarke, B., Uken, R., Reinhardt, J., Jul. 2009. Structural and compositional constraints on the
967 emplacement of the Bushveld Complex, South Africa. Lithos 111 (1-2), 21–36.

- 968 Corcoran, P. L., Bumby, A. J., Davis, D. W., 2013. The Paleoproterozoic Waterberg Group, South
969 Africa: Provenance and its relation to the timing of the Limpopo orogeny. *Precambrian Research*
970 230, 45–60.
- 971 Dorland, H. C., Beukes, N. J., Gutzmer, J., Evans, D. A. D., Armstrong, R. A., 2006. Precise
972 SHRIMP U-Pb zircon age constraints on the lower Waterberg and Soutpansberg Groups, South
973 Africa. *South African Journal of Geology* 109 (1-2), 139–156.
- 974 Eales, H. V., Cawthorn, R. G., 1996. The Bushveld Complex. In: *Layered Intrusions*. Elsevier, pp.
975 181–229.
- 976 Finn, C. A., Bedrosian, P. A., Cole, J. C., Khoza, T. D., Webb, S. J., 2015. Mapping the 3D
977 extent of the Northern Lobe of the Bushveld layered mafic intrusion from geophysical data.
978 *Precambrian Research* 268, 279–294.
- 979 Good, N., de Wit, M. J., Feb. 1997. The Thabazimbi-Murchison Lineament of the Kaapvaal Craton,
980 South Africa: 2700 Ma of episodic deformation. *Journal of the Geological Society* 154 (1), 93–97.
- 981 Grobler, D. F., Nielsen, S. A., Broughton, D., 2012. Upper Critical Zone (Merensky Reef- UG2)
982 correlates within the Platreef on Turspruit Farm, northern limb, Bushveld Complex. In: 6th
983 Platreef Workshop 8th-10th May 2015.
- 984 Harmer, R. E., Pillay, N., Davis, P. G., 2004. The Aurora Project - Main Zone hosted PGE-base
985 metal mineralisation at the northern outcrop limit of the Bushveld Northern Limb, north of
986 Mokopane. In: 1st Platreef Workshop, 16-19 July.
- 987 Holwell, D. A., Armitage, P. E. B., McDonald, I., Dec. 2005. Observations on the relationship
988 between the Platreef and its hangingwall. *Applied Earth Science* 114 (4), 199–207.
- 989 Holwell, D. A., Jones, A., Smith, J. W., Boyce, A. J., 2013. New mineralogical and isotopic con-
990 straints on Main Zone-hosted PGE mineralisation at Moorddrift, northern Bushveld Complex.
991 *Mineralium Deposita* 48 (6), 675–686.
- 992 Holwell, D. A., Jordaan, A., Jun. 2006. Three-dimensional mapping of the Platreef at the Zwart-
993 fontein South mine: implications for the timing of magmatic events in the northern limb of the
994 Bushveld Complex, South Africa. *Applied Earth Science* 115 (2), 41–48.
- 995 Holwell, D. A., McDonald, I., Aug. 2006. Petrology, geochemistry and the mechanisms determining
996 the distribution of platinum-group element and base metal sulphide mineralisation in the Platreef
997 at Overysel, northern Bushveld Complex, South Africa. *Mineralium Deposita* 41 (6), 575–598.
- 998 Holzer, L., Frei, R., Barton Jr., J. M., Kramers, J. D., Jan. 1998. Unraveling the record of successive
999 high grade events in the Central Zone of the Limpopo Belt using Pb single phase dating of
1000 metamorphic minerals. *Precambrian Research* 87 (1-2), 87–115.
- 1001 Hon, K., Kauahikaua, J., Denlinger, R., Mackay, K., 1994. Emplacement and inflation of pahoehoe
1002 sheet flows: Observations and measurements of active lava flows on Kilauea Volcano, Hawaii.
1003 *Geological Society of America Bulletin* 106 (3), 351–370.
- 1004 Huber, H., Koeberl, C., McDonald, I., Reimold, W. U., 2001. Geochemistry and petrology of Wit-
1005 watersrand and Dwyka diamictites from South Africa: search for an extraterrestrial component.
1006 *Geochimica et Cosmochimica Acta* 65 (12), 2007–2016.

- 1007 Hulbert, L. J., von Gruenewaldt, G., 1982. Nickel, copper, and platinum mineralization in the lower
1008 zone of the Bushveld Complex, south of Potgietersrus. *Economic Geology* 77 (6), 1296–1306.
- 1009 Hulbert, L. J., von Gruenewaldt, G., 1985. Textural and compositional features of chromite in
1010 the lower and critical zones of the Bushveld Complex south of Potgietersrus. *Economic Geology*
1011 80 (4), 872–895.
- 1012 Hutchinson, D., Kinnaird, J. A., 2005. Complex multistage genesis for the Ni–Cu–PGE minerali-
1013 sation in the southern region of the Platreef, Bushveld Complex, South Africa. *Applied Earth*
1014 *Science* 114 (4), 208–224.
- 1015 Huthmann, F. M., Yudovskaya, M. A., Frei, D., Kinnaird, J. A., 2016. Geochronological evidence
1016 for an extension of the Northern Lobe of the Bushveld Complex, Limpopo Province, South
1017 Africa. *Precambrian Research* 280, 61–75.
- 1018 Kinnaird, J. A., Dec. 2005. Geochemical evidence for multiphase emplacement in the southern
1019 Platreef. *Applied Earth Science* 114 (4), 225–242.
- 1020 Kinnaird, J. A., Hutchinson, D., Schurmann, L., Nex, P. A. M., de Lange, R., 2005. Petrology and
1021 mineralisation of the southern Platreef: northern limb of the Bushveld Complex, South Africa.
1022 *Mineralium Deposita* 40 (5), 576–597.
- 1023 Kinnaird, J. A., Nex, P. A. M., 2015. An Overview of the Platreef. In: *Platinum-group element*
1024 *(PGE) mineralisation and resources of the Bushveld Complex, South Africa. An Overview of the*
1025 *Platreef*, Council for Geoscience, South Africa, pp. 193–342.
- 1026 Kinnaird, J. A., Yudovskaya, M. A., Botha, M. J., 2014. The Waterberg Extension to the Bushveld
1027 Complex. In: *11th International Platinum Symposium*. Yekaterinburg, Russia.
- 1028 Kinnaird, J. A., Yudovskaya, M. A., McCreesh, M. J. G., Huthmann, F. M., Botha, T. J., 2017.
1029 The Waterberg PGE Deposit - atypical mineralization in mafic-ultramafic rocks of the Bushveld
1030 Complex, South Africa. *Economic Geology* 112, 1367–1394.
- 1031 Kramers, J. D., Mouri, H., 2011. The geochronology of the Limpopo Complex: A controversy
1032 solved. In: van Reenen, D. D., Kramers, J. D., McCourt, S., Perchuk, L. L. (Eds.), *Origin and*
1033 *Evolution of Precambrian High-grade Gneiss Terranes, with Special Emphasis on the Limpopo*
1034 *Complex of Southern Africa*. Geological Society of America Memoir, pp. 85–106.
- 1035 Kruger, F. J., 2005. Filling the Bushveld Complex magma chamber: lateral expansion, roof and
1036 floor interaction, magmatic unconformities, and the formation of giant chromitite, PGE and
1037 Ti-V-magnetite deposits. *Mineralium Deposita* 40 (5), 451–472.
- 1038 Lee, C. A., 1996. A review of mineralization in the Bushveld Complex and some other layered
1039 intrusions. In: *Layered Intrusions*. Elsevier, pp. 103–145.
- 1040 Lightfoot, P. C., Evans-Lamswood, D., 2015. Structural controls on the primary distribution of
1041 mafic-ultramafic intrusions containing Ni–Cu–Co–(PGE) sulfide mineralization in the roots of
1042 large igneous provinces. *Ore Geology Reviews* 64 (C), 354–386.
- 1043 Lodders, K., Jul. 2003. Solar System Abundances and Condensation Temperatures of the Elements.
1044 *The Astrophysical Journal* 591 (2), 1220–1247.
- 1045 Maier, W. D., Barnes, S.-J., 1998. Concentrations of rare earth elements in silicate rocks of the
1046 Lower, Critical and Main Zones of the Bushveld Complex. *Chemical Geology* 150 (1-2), 85–103.

- 1047 Maier, W. D., Barnes, S.-J., Nov. 1999. Platinum-Group Elements in Silicate Rocks of the Lower,
1048 Critical and Main Zones at Union Section, Western Bushveld Complex. *Journal of Petrology*
1049 40 (11), 1647–1671.
- 1050 Maier, W. D., Barnes, S.-J., Sep. 2008. Platinum-group elements in the UG1 and UG2 chromi-
1051 tites, and the Bastard reef, at Impala platinum mine, western Bushveld Complex, South Africa:
1052 Evidence for late magmatic cumulate instability and reef constitution. *South African Journal of*
1053 *Geology* 111 (2-3), 159–176.
- 1054 Maier, W. D., Barnes, S.-J., 2010. The petrogenesis of platinum-group element reefs in the Upper
1055 Main Zone of the Northern Lobe of the Bushveld Complex on the farm Moorddrift, South Africa.
1056 *Economic Geology*.
- 1057 Maier, W. D., De Klerk, L., Blaine, J., Manyeruke, T., Barnes, S.-J., Stevens, M. V. A., Mavro-
1058 genes, J. A., 2008. Petrogenesis of contact-style PGE mineralization in the northern lobe of the
1059 Bushveld Complex: comparison of data from the farms Rooipoort, Townlands, Drenthe and
1060 Nonnenwerth. *Mineralium Deposita* 43 (3), 255–280.
- 1061 Manyeruke, T. D., Mar. 2007. Compositional and lithological variation of the Platreef on the farm
1062 Nonnenwerth, northern lobe of the Bushveld Complex: Implications for the origin of Platinum-
1063 group elements (PGE) mineralization . Ph.D. thesis, University of Pretoria.
- 1064 McDonald, I., Harmer, R., Holwell, D. A., Hughes, H. S. R., Boyce, A. J., 2017. Cu-Ni-PGE
1065 mineralisation at the Aurora Project and potential for a new PGE province in the Northern
1066 Bushveld Main Zone. *Ore Geology Reviews* 80, 1135–1159.
- 1067 McDonald, I., Harmer, R. E., 2010. The Nature of PGE mineralization in the Aurora Project
1068 Area, Northern Bushveld Complex, South Africa. In: JUGO, P. J., Leshner, C. M., Mungall,
1069 J. E. (Eds.), 11th International Platinum Symposium.
- 1070 McDonald, I., Holwell, D. A., 2011. Geology of the northern Bushveld Complex and the setting and
1071 genesis of the Platreef Ni–Cu–PGE deposit. In: *Reviews in Economic Geology* v. 17. *Reviews in*
1072 *Economic Geology*, pp. 297–327.
- 1073 McDonald, I., Holwell, D. A., Armitage, P. E. B., Dec. 2005. Geochemistry and mineralogy of
1074 the Platreef and “Critical Zone” of the northern lobe of the Bushveld Complex, South Africa:
1075 implications for Bushveld stratigraphy and the development of PGE mineralisation. *Mineralium*
1076 *Deposita* 40 (5), 526–549.
- 1077 McDonald, I., Holwell, D. A., Wesley, B., Mar. 2009. Assessing the potential involvement of an early
1078 magma staging chamber in the generation of the Platreef Ni–Cu–PGE deposit in the northern
1079 limb of the Bushveld Complex: a pilot study of the Lower Zone Complex at Zwartfontein.
1080 *Applied Earth Science* 118 (1), 5–20.
- 1081 McDonald, I., Viljoen, K. S., 2006. Platinum-group element geochemistry of mantle eclogites: a
1082 reconnaissance study of xenoliths from the Orapa kimberlite, Botswana. *Applied Earth Science*
1083 115 (3), 81–93.
- 1084 Mitchell, A. A., Scoon, R. N., 2012. The Platreef of the Bushveld Complex, South Africa: Non-
1085 sequential Magma Replenishment Based on Observations at the Akanani Project, North-west of
1086 Mokopane. *South African Journal of Geology* 115 (4), 535–550.

- 1087 Molyneux, T. G., 1974. A geological investigation of the Bushveld Complex in Sekhukhuneland and
1088 part of the Steelpoort valley. *Transactions of the Geological Society of South Africa*, 329–338.
- 1089 Mungall, J. E., Brenan, J. M., Jan. 2014. Partitioning of platinum-group elements and Au between
1090 sulfide liquid and basalt and the origins of mantle-crust fractionation of the chalcophile elements.
1091 *Geochimica et Cosmochimica Acta* 125 (C), 265–289.
- 1092 Naldrett, A., Kinnaird, J. A., Wilson, A. H., Yudovskaya, M. A., Chunnett, G., 2011. Genesis of
1093 the PGE-enriched Merensky Reef and chromitite seams of the Bushveld Complex: . In: *Reviews*
1094 *in Economic Geology* v. 17. Society of Economic Geologists, pp. 235–296.
- 1095 Naldrett, A. J., May 2010. Secular Variation of Magmatic Sulfide Deposits and Their Source
1096 Magmas. *Economic Geology* 105 (3), 669–688.
- 1097 Nicoli, G., Stevens, G., Moyen, J. F., Frei, D., 2015. Rapid evolution from sediment to anatectic
1098 granulite in an Archean continental collision zone: the example of the Bandelierkop Formation
1099 metapelites, South Marginal Zone, Limpopo Belt, South Africa. *Journal of Metamorphic Geology*
1100 33 (2), 177–202.
- 1101 Rajesh, H. M., Santosh, M., Wan, Y., Liu, D., Liu, S. J., Belyanin, G. A., Mar. 2014. Ultrahigh
1102 temperature granulites and magnesian charnockites: Evidence for Neoproterozoic accretion along
1103 the northern margin of the Kaapvaal Craton. *Precambrian Research* 246, 150–159.
- 1104 Renna, M. R., Tribuzio, R., Aug. 2011. Olivine-rich Troctolites from Ligurian Ophiolites (Italy):
1105 Evidence for Impregnation of Replacive Mantle Conduits by MORB-type Melts. *Journal of*
1106 *Petrology* 52 (9), 1763–1790.
- 1107 Robertson, J., Ripley, E. M., Barnes, S. J., Li, C., 2015. Sulfur Liberation from Country Rocks
1108 and Incorporation in Mafic Magmas. *Economic Geology* 110 (4), 1111–1123.
- 1109 Roelofse, F., Ashwal, L. D., 2012. The Lower Main Zone in the Northern Limb of the Bushveld
1110 Complex—a >1.3 km Thick Sequence of Intruded and Variably Contaminated Crystal Mushes.
1111 *Journal of Petrology* 53 (7), 1449–1476.
- 1112 Saper, L., Liang, Y., 2014. Formation of plagioclase-bearing peridotite and plagioclase-bearing
1113 wehrlite and gabbro suite through reactive crystallization: an experimental study. *Contributions*
1114 *to Mineralogy and Petrology* 167:985.
- 1115 Schaller, M., Steiner, O., Studer, I., Holzer, L., Herwegh, M., Jun. 1999. Exhumation of Limpopo
1116 Central Zone granulites and dextral continent-scale transcurrent movement at 2.0 Ga along the
1117 Palala Shear Zone, Northern Province, South Africa. *Precambrian Research* 96, 263–288.
- 1118 Scoates, J. S., Friedman, R. M., 2008. Precise Age of the Platiniferous Merensky Reef, Bushveld
1119 Complex, South Africa, by the U-Pb Zircon Chemical Abrasion ID-TIMS Technique. *Economic*
1120 *Geology* 103 (3), 465–471.
- 1121 Scoates, J. S., Wall, C. J., 2015. Geochronology of Layered Intrusions. In: Charlier, B., Namur, O.,
1122 Latypov, R., Tegner, C. (Eds.), *Layered Intrusions*. Springer Netherlands, Dordrecht, pp. 3–74.
- 1123 Seabrook, C. L., Cawthorn, R. G., Kruger, F. J., 2005. The Merensky Reef, Bushveld Complex:
1124 mixing of minerals not mixing of magmas. *Economic Geology* 100, 1191–1206.

- 1125 Smirnov, A. V., Evans, D. A. D., Ernst, R. E., Söderlund, U., Li, Z.-X., Jan. 2013. Trading
1126 partners: Tectonic ancestry of southern Africa and western Australia, in Archean supercratons
1127 Vaalbara and Zimgarn. *Precambrian Research* 224, 11–22.
- 1128 Smit, C. A., Roering, C., van Reenen, D. D., 1992. The structural framework of the southern margin
1129 of the Limpopo Belt, South Africa. In: van Reenen, D. D., Roering, C., Ashwal, L. D., de Wit,
1130 M. J. (Eds.), *The Archean Limpopo Granulite Belt: Tectonics and Deep Crustal Processes*.
1131 *Precambrian Research*, pp. 51–67.
- 1132 Sun, S. S., McDonough, W. F., 1989. Chemical and isotopic systematics of oceanic basalts: impli-
1133 cations for mantle composition and processes. *Geological Society, London, Special Publications*
1134 42 (1), 313–345.
- 1135 Tanner, D., Mavrogenes, J. A., Arculus, R. J., Jenner, F. E., 2014. Trace Element Stratigraphy
1136 of the Bellevue Core, Northern Bushveld: Multiple Magma Injections Obscured by Diffusive
1137 Processes. *Journal of Petrology* 55 (5), 859–882.
- 1138 Treloar, P. J., Coward, M. P., Harris, N. B. W., 1992. Himalayan-Tibetan analogies for the evolution
1139 of the Zimbabwe Craton and Limpopo Belt. *Precambrian Research* 55 (1-4), 571–587.
- 1140 van der Merwe, M. J., 1976. The layered sequence of the Potgietersrus Limb of the Bushveld
1141 Complex. *Economic Geology* 71 (7), 1337–1351.
- 1142 van Reenen, D. D., Barton, J. M., Roering, C., Smith, C. A., Van Schalkwyk, J. F., 1987. Deep
1143 crystal response to continental collision: The Limpopo belt of southern Africa. *Geology* 15 (1),
1144 11.
- 1145 von Gruenewaldt, G., Sharpe, M. R., Hatton, C. J., 1985. The Bushveld Complex; introduction
1146 and review. *Economic Geology* 80 (4), 803–812.
- 1147 Walraven, F., 1997. Geochronology of the Rooiberg Group, Transvaal Supergroup, South Africa.
1148 , Information Circular No. 316, *Economic Geology Research Unit, University of the Witwater-*
1149 *srand*.
- 1150 Walraven, F., Hattingh, E., 1993. Geochronology of the Nebo Granite, Bushveld Complex. *South*
1151 *African Journal of Geology* 96 (1/2), 31–41.
- 1152 Webb, S. J., Cawthorn, R. G., Nguuri, T., James, D., Jun. 2004. Gravity modeling of Bushveld
1153 Complex connectivity supported by Southern African Seismic Experiment results. *South African*
1154 *Journal of Geology* 107 (1-2), 207–218.
- 1155 Wiebe, R. A., 1980. Commingling of contrasted magmas in the plutonic environment: examples
1156 from the Nain anorthositic complex. *The Journal of Geology* 88 (2), 197–209.
- 1157 Willemsse, J., 1969. The geology of the Bushveld Igneous Complex, the largest repository of mag-
1158 matic ore deposits in the world. In: *Magmatic Ore Deposits - A Symposium*. pp. 1–22.
- 1159 Wilson, A. H., May 2012. A Chill Sequence to the Bushveld Complex: Insight into the First
1160 Stage of Emplacement and Implications for the Parental Magmas. *Journal of Petrology* 53 (6),
1161 1123–1168.
- 1162 Yudovskaya, M. A., Kinnaird, J. A., Grobler, D. F., Costin, G., Abramova, V. D., Dunnett,
1163 T., Barnes, S.-J., 2017. Zonation of Merensky-Style Platinum-Group Element Mineralization in
1164 Turfspruit Thick Reef Facies (Northern Limb of the Bushveld Complex). *Economic Geology* 112.

- 1165 Yudovskaya, M. A., Kinnaird, J. A., McCreesh, M. J. G., Frei, D., 2015. The lithology at the
1166 contact between the Bushveld Mafic–Ultramafic sequence and overlying Waterberg sediments on
1167 the Waterberg. In: 6th Platreef Workshop 8th-10th May 2015. pp. 59–61.
- 1168 Yudovskaya, M. A., Kinnaird, J. A., Naldrett, A. J., Mokhov, A. V., McDonald, I., Reinke, C.,
1169 2011. Facies Variation in PGE Mineralization in the Central Platreef of the Bushveld Complex,
1170 South Africa. *The Canadian Mineralogist* 49 (6), 1349–1384.
- 1171 Yudovskaya, M. A., Kinnaird, J. A., Naldrett, A. J., Rodionov, N., Antonov, A., Simakin, S.,
1172 Kuzmin, D., 2013a. Trace-element study and age dating of zircon from chromitites of the
1173 Bushveld Complex (South Africa). *Mineralogy and Petrology* 107 (6), 915–942.
- 1174 Yudovskaya, M. A., Kinnaird, J. A., Sobolev, A. V., Kuzmin, D. V., McDonald, I., Wilson, A. H.,
1175 2013b. Petrogenesis of the Lower Zone olivine-rich cumulates beneath the Platreef and their
1176 correlation with recognized occurrences in the Bushveld Complex. *Economic Geology* 108, 1923–
1177 1952.
- 1178 Zeh, A., Ovtcharova, M., Wilson, A. H., Schaltegger, U., 2015. The Bushveld Complex was em-
1179 placed and cooled in less than one million years – results of zirconology, and geotectonic impli-
1180 cations. *Earth and Planetary Science Letters* 418, 103–114.

Table 1: Representative geochemical results for rocks analyzed during this study.

Sample ID	UZ1	UZ2	UZ3	UZ4	MZ1	MZ2	MZ3	MZ4	MZ5	MZ6	MZ7	MZ8	MZ9	MZ10	TR1	TR2	TR3	TR4
Rock Type	FEGB	FEGB	FEGB	FEGN	GN	T peg N	T PX	opx TR	peg TR	TR	TR							
Group	UZ	UZ	UZ	UZ	MZ	MZ	MZ	TR	TR	TR	TR							
XRF %																		
SiO2	51.34	51.22	51.83	51.18	50.44	51.55	51.35	51.11	51.86	50.14	50.23	50.93	50.42	49.39	43.21	47.72	43.58	44.40
Al2O3	12.43	16.96	17.50	18.98	19.02	18.13	15.96	19.16	13.33	24.36	21.24	18.49	20.62	26.53	8.43	13.05	6.39	9.11
Fe2O3	10.26	8.44	8.17	6.70	7.08	7.76	8.59	6.78	9.37	4.25	6.03	7.77	9.13	6.19	15.83	10.39	16.66	13.10
MnO	0.18	0.15	0.15	0.13	0.13	0.14	0.16	0.12	0.18	0.08	0.11	0.14	0.14	0.07	0.22	0.12	0.22	0.19
MgO	13.28	8.98	9.63	7.55	10.06	8.30	12.94	10.13	15.83	4.89	7.00	8.90	8.18	2.87	27.65	21.48	29.67	28.79
CaO	11.72	12.98	11.85	13.38	11.68	12.91	9.82	11.70	8.51	14.09	13.56	12.06	10.50	12.19	4.90	7.49	4.39	5.14
Na2O	0.88	1.69	1.82	2.02	1.48	1.92	1.33	1.62	1.07	2.18	1.77	1.79	2.01	2.84	0.51	0.73	0.61	0.35
K2O	0.22	0.15	0.12	0.15	0.11	0.11	0.13	0.11	0.12	0.12	0.11	0.12	0.21	0.22	0.07	0.11	0.08	0.12
TiO2	0.21	0.23	0.17	0.18	0.14	0.16	0.16	0.12	0.13	0.14	0.15	0.20	0.14	0.17	0.14	0.11	0.10	0.08
P2O5	0.02	0.02	0.02	0.02	0.02	0.02	0.02	0.02	0.02	0.02	0.02	0.02	0.02	0.02	0.10	0.02	0.02	0.02
Cr2O3	0.06	0.03	0.02	0.02	0.11	0.03	0.12	0.10	0.14	0.05	0.06	0.03	0.01	0.00	0.62	0.10	0.04	0.10
NiO	0.03	0.02	0.02	0.02	0.03	0.02	0.03	0.04	0.04	0.01	0.02	0.02	0.10	0.33	0.18	0.17	0.21	0.18
LOI	3.23	1.38	0.43	0.66	0.46	0.47	0.35	0.47	0.58	0.55	0.47	1.25	1.13	1.48	5.30	5.56	5.39	7.34
Total	99.72	100.12	100.57	99.73	99.66	100.37	99.84	100.38	99.75	99.93	99.75	99.78	100.66	100.34	100.34	100.55	100.49	100.40
S ppm XRF	196	361	NA	172	NA	NA	NA	41	39	95	NA	NA	2731	12786	466	1146	467	269
ICP-MS ppm																		
Li	3.27	2.37	2.06	1.99	2.07	1.35	2.39	3.22	1.03	1.21	2.22	3.19	1.95	2.76	1.45	0.75	3.26	1.56
P	35.08	66.22	40.14	52.69	61.93	21.22	65.47	39.58	33.92	40.68	60.15	71.17	28.60	400.53	63.48	45.03	59.58	31.79
Sc	21.02	17.66	14.57	14.90	12.89	16.35	7.35	10.07	11.76	6.84	9.95	9.09	8.87	1.63	11.04	9.65	7.12	6.56
Ti	1177.14	1567.47	1095.39	1278.42	845.51	811.62	764.64	556.25	605.09	675.87	795.64	1242.24	665.33	804.89	785.45	452.36	402.58	253.98
V	162.31	163.79	133.68	135.28	93.66	129.91	90.92	87.00	94.35	77.85	109.44	110.57	74.13	37.53	94.56	48.63	41.93	35.40
Cr	297.94	162.72	59.75	94.37	632.59	612.41	495.62	632.01	646.01	225.39	301.40	129.36	68.15	7.47	3493.35	391.13	166.84	505.57
Co	60.06	46.99	70.40	55.73	39.81	54.61	57.20	47.39	69.00	24.23	35.94	67.12	65.63	75.55	193.28	114.69	157.70	130.69
Ni	209.37	162.84	175.56	125.56	183.63	501.27	225.06	238.08	228.36	96.46	120.75	163.50	680.41	1949.27	1136.85	1041.82	1372.40	1070.04
Cu	62.70	34.16	69.73	36.97	30.83	48.11	24.37	33.59	26.73	22.48	23.98	33.82	808.77	3251.31	20.63	99.13	37.77	6.64
Zn	59.34	48.73	62.10	49.23	41.63	50.85	52.07	41.69	55.19	24.64	35.76	64.14	55.68	104.01	109.74	50.65	89.92	64.36
Ga	7.69	10.77	13.42	15.01	10.02	12.04	9.60	10.93	7.79	13.53	12.30	13.60	11.42	14.23	7.41	7.64	4.00	4.68
As	0.30	0.36	0.20	0.30	0.31	0.24	0.17	0.21	0.20	0.20	0.21	0.33	0.32	0.26	0.40	0.25	0.18	0.15
Rb	3.64	1.30	0.93	1.55	1.38	0.66	1.88	0.64	1.78	0.49	0.73	1.30	2.42	1.72	2.70	3.75	1.66	3.63
Sr	44.07	107.61	99.20	129.34	104.30	121.14	94.87	110.46	79.34	123.46	112.43	105.81	106.22	85.03	56.33	143.97	52.63	67.33
Y	6.22	4.16	2.97	2.93	2.43	3.22	1.36	1.77	1.56	1.39	2.10	1.85	1.69	1.34	2.03	2.05	1.52	1.24
Zr	8.28	13.05	10.61	14.04	10.31	5.60	6.09	5.51	4.22	6.02	7.90	12.69	6.71	8.49	12.51	8.82	3.64	4.47
Nb	0.27	0.64	0.38	0.49	1.14	0.14	0.26	0.19	0.16	0.20	0.20	0.73	0.20	0.66	0.35	0.26	0.15	0.19
Ba	36.63	32.30	32.55	38.13	26.29	28.24	29.16	28.64	36.80	23.42	23.56	31.40	38.90	18.27	26.24	36.72	26.03	38.80
Sn	0.24	1.14	0.64	3.34	0.41	0.43	0.27	0.38	0.16	0.25	0.32	0.60	0.33	0.54	0.59	0.26	0.19	0.15
Cs	0.17	0.07	0.05	0.05	0.07	0.03	0.06	0.07	0.11	0.02	0.03	0.05	0.21	0.15	0.22	0.45	0.26	0.31
La	1.45	1.82	1.14	1.28	1.19	0.95	1.20	0.87	0.95	0.91	1.28	1.50	0.91	1.20	1.07	1.26	1.01	0.97
Ce	3.09	4.69	2.39	3.19	2.57	2.71	2.50	2.26	1.85	2.48	2.83	3.05	2.81	4.18	1.64	2.31	1.56	1.57
Pr	0.39	0.49	0.28	0.30	0.25	0.25	0.22	0.18	0.18	0.20	0.26	0.29	0.20	0.33	0.25	0.27	0.18	0.17
Nd	1.86	2.26	1.30	1.40	1.12	1.24	0.91	0.81	0.77	0.88	1.15	1.22	0.88	1.44	1.05	1.17	0.81	0.73
Sm	0.53	0.59	0.37	0.39	0.29	0.37	0.20	0.22	0.19	0.22	0.29	0.28	0.22	0.30	0.25	0.29	0.21	0.18
Eu	0.22	0.23	0.16	0.17	0.15	0.16	0.14	0.13	0.12	0.14	0.15	0.17	0.15	0.09	0.13	0.14	0.11	0.11
Gd	0.63	0.68	0.46	0.48	0.34	0.46	0.22	0.26	0.22	0.26	0.34	0.35	0.26	0.34	0.28	0.30	0.23	0.18
Tb	0.11	0.11	0.08	0.08	0.06	0.08	0.03	0.05	0.04	0.04	0.05	0.05	0.04	0.05	0.05	0.05	0.04	0.03
Dy	0.79	0.77	0.57	0.54	0.42	0.58	0.25	0.32	0.27	0.27	0.38	0.35	0.30	0.29	0.34	0.35	0.27	0.21
Ho	0.17	0.16	0.13	0.12	0.09	0.13	0.05	0.07	0.06	0.06	0.08	0.07	0.07	0.06	0.07	0.08	0.06	0.05
Er	0.49	0.47	0.36	0.34	0.28	0.38	0.15	0.21	0.19	0.16	0.23	0.22	0.20	0.15	0.22	0.22	0.17	0.14
Tm	0.07	0.07	0.06	0.05	0.04	0.06	0.02	0.03	0.03	0.03	0.03	0.04	0.03	0.02	0.03	0.03	0.03	0.02
Yb	0.53	0.45	0.37	0.33	0.30	0.39	0.17	0.24	0.22	0.16	0.23	0.22	0.23	0.14	0.23	0.24	0.19	0.16
Lu	0.08	0.07	0.06	0.05	0.05	0.06	0.03	0.04	0.04	0.03	0.04	0.03	0.04	0.02	0.04	0.04	0.03	0.03
Hf	0.27	0.39	0.31	0.41	0.26	0.19	0.17	0.16	0.12	0.17	0.21	0.33	0.20	0.25	0.27	0.22	0.10	0.11
Ta	0.02	0.04	0.03	0.03	0.10	0.01	0.02	0.01	0.01	0.02	0.02	0.05	0.01	0.04	0.03	0.01	0.03	0.03
W	0.03	0.04	0.03	0.03	0.04	0.06	0.03	0.02	0.02	0.03	0.03	0.04	0.02	0.02	0.08	0.02	0.15	0.09
Pb	1.60	0.97	2.05	2.41	0.65	0.95	0.58	0.75	0.62	0.70	0.89	2.08	2.83	14.28	2.68	2.76	1.07	1.71
Th	0.11	0.22	0.13	0.18	0.13	0.07	0.13	0.10	0.11	0.08	0.10	0.16	0.15	0.21	0.16	1.15	0.07	0.08
U	0.04	0.08	0.08	0.10	0.05	0.03	0.06	0.05	0.04	0.04	0.04	0.11	0.06	0.12	0.07	0.12	0.03	0.06
PGE ppb																		
Os	0.29	0.13	NA	0.11	NA	NA	NA	0.07	0.21	0.06	NA	NA	29.7	1.59	0.05	0.23	0.24	0.09
Ir	0.52	0.09	NA	0.10	NA	NA	NA	0.17	0.95	0.55	NA	NA	29.2	5.65	0.04	0.35	0.30	0.13
Ru	0.35	0.21	NA	0.23	NA	NA	NA	0.49	1.08	0.38	NA	NA	115	11.3	0.20	1.11	0.91	0.53
Rh	3.26	0.54	NA	0.53	NA	NA	NA	0.93	3.70	2.53	NA	NA	85.3	12.3	0.53	1.77	1.87	0.99
Pt	20.																	

Sample ID	TR5	TR6	TR7	TR8	TR9	TR10	TR11	TR12	HZ1	HZ2	HZ3	HZ4	HZ5	HZ6	HZ7	HZ8	HZ9	HZ10
Rock Type	TR	TR	TR	TR	TR	TR	TR	TR	DUN/HZ	HZ-serp								
Group	TR	TR	TR	TR	TR	TR	TR	TR	HZ									
XRF %	TR	TR	TR	TR	TR	TR	TR	TR	HZ									
SiO2	44.02	42.89	45.04	44.35	39.74	45.86	44.25	45.71	44.72	43.71	46.24	48.11	51.56	49.17	49.23	51.90	43.35	45.03
Al2O3	10.97	6.68	14.29	12.81	10.51	10.03	8.77	21.48	7.26	6.28	6.76	6.41	6.08	15.62	9.26	6.74	10.92	13.39
Fe2O3	12.26	18.33	11.65	12.87	15.94	13.15	13.23	7.48	16.01	17.56	14.95	13.66	10.20	9.02	14.18	13.61	13.51	12.58
MnO	0.17	0.24	0.16	0.18	0.20	0.20	0.17	0.10	0.23	0.22	0.22	0.22	0.16	0.15	0.19	0.22	0.20	0.17
MgO	26.34	28.16	20.61	21.62	25.23	23.83	28.99	13.83	26.86	26.77	27.70	27.64	25.95	14.00	21.22	24.24	25.28	19.24
CaO	6.14	4.83	8.44	7.73	5.47	6.85	5.04	10.97	5.46	5.20	4.16	4.17	5.59	10.29	5.49	3.76	7.02	9.12
Na2O	0.39	0.35	0.70	0.83	0.45	0.59	0.47	1.18	0.65	0.49	0.55	0.47	0.42	1.45	0.93	0.21	0.53	0.79
K2O	0.18	0.08	0.27	0.06	0.09	0.07	0.13	0.19	0.14	0.13	0.10	0.13	0.08	0.18	0.30	0.14	0.41	0.27
TiO2	0.06	0.07	0.06	0.07	0.17	0.12	0.07	0.05	0.08	0.11	0.11	0.12	0.10	0.16	0.21	0.22	0.07	0.06
P2O5	0.02	0.02	0.02	0.02	0.02	0.02	0.02	0.02	0.02	0.02	0.02	0.01	0.02	0.02	0.03	0.02	0.02	0.02
Cr2O3	0.06	0.03	0.09	0.08	2.41	0.52	0.13	0.02	0.06	0.08	0.10	0.32	0.28	0.10	0.09	0.30	0.04	0.07
NiO	0.17	0.22	0.12	0.14	0.17	0.15	0.19	0.10	0.23	0.62	0.31	0.19	0.39	0.46	0.28	0.14	0.23	0.43
LOI	6.60	6.46	5.93	5.45	6.47	5.83	9.14	6.47	4.62	4.91	7.51	3.22	3.33	2.26	4.51	5.61	10.13	4.39
Total	99.67	100.24	100.39	99.59	98.95	100.21	100.27	100.44	100.29	99.61	99.86	100.20	99.93	99.81	100.14	100.27	100.36	100.05
S ppm XRF	NA	721	NA	NA	499	NA	NA	NA	NA	11935	2493	1248	6580	9928	8000	525	1044	9442
ICP-MS ppm																		
Li	2.58	2.66	2.22	1.84	2.01	1.92	0.91	7.92	3.28	1.38	2.16	1.37	3.88	5.71	4.72	3.79	4.86	2.18
P	56.53	29.83	24.60	31.13	30.67	13.53	30.21	20.90	26.87	62.32	50.58	32.88	21.54	46.99	83.19	59.74	20.43	15.59
Sc	7.62	7.93	8.62	10.77	9.44	13.00	7.03	1.70	9.00	9.43	11.46	12.85	15.44	9.35	15.38	19.11	7.53	7.63
Ti	269.05	252.65	284.68	346.79	437.16	638.26	310.53	262.86	513.37	535.98	557.96	612.95	467.20	733.83	1051.95	1352.20	274.05	245.32
V	32.09	36.62	41.77	49.20	79.38	82.32	32.86	16.44	53.82	63.97	49.45	70.05	67.29	72.66	74.88	101.64	36.37	44.24
Cr	316.68	91.64	351.49	462.63	5598.44	2606.25	580.25	50.59	238.54	318.08	370.93	1378.88	1241.13	500.13	416.92	1643.24	280.91	322.41
Co	135.57	148.71	103.73	117.47	108.67	144.09	173.25	104.44	188.62	191.68	195.57	99.23	110.82	97.48	112.33	102.20	115.95	135.46
Ni	1023.52	1271.49	630.69	862.13	928.64	878.10	1052.88	661.21	1495.61	4062.16	1819.59	930.41	2498.85	2963.47	1839.36	796.96	1282.99	2616.62
Cu	10.68	60.70	45.65	44.66	23.45	39.55	7.11	49.81	184.85	2507.57	453.47	233.49	975.01	2114.10	1169.29	61.51	171.33	1157.92
Zn	66.08	109.24	61.50	62.54	63.46	95.41	86.37	50.99	115.65	102.36	96.91	61.12	69.04	48.77	75.61	113.88	81.89	61.30
Ga	5.86	4.02	6.87	6.87	5.53	8.04	5.58	10.08	5.49	3.82	5.77	4.10	4.09	8.22	7.22	7.63	5.20	6.39
As	0.19	0.17	0.21	0.21	0.16	0.28	0.35	0.32	0.35	0.17	0.32	0.18	0.32	0.36	0.30	1.47	0.69	0.18
Rb	4.59	2.17	4.32	0.80	2.52	2.50	6.29	4.93	4.41	2.78	4.92	3.64	3.46	3.00	22.50	8.50	12.68	4.68
Sr	95.63	66.29	93.99	87.83	64.01	64.30	61.58	228.31	57.50	54.94	63.24	46.20	62.86	270.68	101.47	24.73	118.38	142.52
Y	1.36	1.42	1.35	1.55	1.42	2.15	1.19	0.42	1.13	1.83	1.88	2.01	2.09	2.07	3.83	4.37	1.24	0.81
Zr	3.87	2.12	2.84	4.47	2.69	6.21	5.38	2.78	3.23	5.42	5.80	4.78	3.85	7.44	19.66	20.51	2.01	1.69
Nb	0.19	0.08	0.09	0.11	0.17	0.37	0.48	0.11	0.12	0.25	0.25	0.63	0.11	0.31	2.48	0.78	0.06	0.08
Ba	40.18	26.07	29.81	20.53	17.14	19.52	28.40	70.94	30.68	71.48	41.79	15.78	16.76	42.56	47.46	26.52	73.90	88.55
Sn	0.22	0.17	0.18	0.21	0.23	0.45	0.25	0.22	0.41	0.81	0.72	0.26	0.44	0.68	0.59	0.55	1.05	0.59
Cs	0.68	0.31	0.31	0.02	0.26	0.09	0.66	0.27	0.25	0.57	1.17	0.32	0.52	0.20	1.76	0.97	2.01	0.49
La	1.08	0.67	0.89	0.85	0.76	1.10	0.91	0.68	0.64	1.15	1.59	0.79	0.92	1.60	2.23	5.40	0.73	0.59
Ce	1.68	1.03	1.49	1.59	1.35	1.85	1.47	1.15	0.91	2.10	2.18	1.27	1.75	3.14	5.06	8.13	1.23	1.04
Pr	0.19	0.13	0.17	0.19	0.16	0.25	0.19	0.12	0.12	0.25	0.26	0.15	0.20	0.33	0.60	1.03	0.14	0.11
Nd	0.81	0.59	0.74	0.81	0.70	1.03	0.78	0.47	0.53	1.08	1.09	0.72	0.82	1.39	2.59	3.93	0.58	0.47
Sm	0.19	0.18	0.19	0.19	0.17	0.26	0.17	0.12	0.15	0.30	0.27	0.20	0.21	0.32	0.63	0.74	0.18	0.16
Eu	0.11	0.10	0.14	0.14	0.10	0.13	0.09	0.12	0.09	0.13	0.14	0.10	0.09	0.19	0.23	0.14	0.14	0.13
Gd	0.21	0.21	0.20	0.22	0.20	0.31	0.19	0.11	0.17	0.28	0.30	0.24	0.25	0.34	0.64	0.82	0.18	0.12
Tb	0.03	0.03	0.04	0.04	0.03	0.05	0.03	0.01	0.03	0.05	0.05	0.04	0.05	0.06	0.10	0.11	0.03	0.02
Dy	0.23	0.25	0.24	0.26	0.24	0.37	0.20	0.08	0.20	0.33	0.32	0.32	0.32	0.37	0.67	0.74	0.21	0.15
Ho	0.05	0.06	0.05	0.06	0.05	0.08	0.04	0.02	0.04	0.07	0.07	0.08	0.08	0.08	0.15	0.16	0.05	0.03
Er	0.15	0.16	0.16	0.17	0.16	0.23	0.13	0.05	0.13	0.19	0.21	0.23	0.23	0.23	0.42	0.49	0.14	0.09
Tm	0.02	0.02	0.02	0.03	0.02	0.04	0.02	0.01	0.02	0.03	0.03	0.04	0.03	0.03	0.06	0.08	0.02	0.01
Yb	0.17	0.18	0.16	0.18	0.17	0.25	0.14	0.05	0.13	0.19	0.22	0.25	0.27	0.25	0.44	0.52	0.16	0.10
Lu	0.03	0.03	0.03	0.03	0.03	0.04	0.02	0.01	0.02	0.03	0.04	0.04	0.04	0.04	0.07	0.09	0.03	0.02
Hf	0.10	0.07	0.08	0.11	0.09	0.18	0.14	0.07	0.10	0.16	0.16	0.14	0.12	0.21	0.60	0.54	0.06	0.05
Ta	0.02	0.00	0.02	0.02	0.01	0.03	0.04	0.01	0.01	0.02	0.04	0.05	0.01	0.02	0.17	0.05	0.00	0.00
W	0.07	0.11	0.02	0.03	0.00	0.03	0.09	0.01	0.11	0.41	0.12	0.02	0.08	0.07	0.18	0.21	0.10	0.08
Pb	0.67	1.59	0.39	0.38	0.92	1.07	2.34	1.13	5.50	9.92	9.67	0.85	2.00	2.67	5.18	1.83	1.02	5.46
Th	0.14	0.04	0.12	0.06	0.06	0.31	0.25	0.05	0.04	0.14	0.11	0.07	0.07	0.15	1.30	0.36	0.04	0.03
U	0.04	0.02	0.04	0.02	0.02	0.09	0.16	0.02	0.03	0.06	0.05	0.02	0.03	0.06	0.69	0.23	0.02	0.02
PGE ppb																		
Os	NA	0.35	NA	NA	22.6	NA	NA	NA	NA	11.2	14.44	1.33	4.32	11.8	4.35	0.53	13.51	11.38
Ir	NA	0.68	NA	NA	40.7	NA	NA	NA	NA	18.0	12.16	1.92	11.6	23.1	6.48	1.00	14.49	18.50
Ru	NA	1.87	NA	NA	102	NA	NA	NA	NA	41.5	45.89	5.87	24.8	53.5	16.8	2.41	50.91	47.81
Rh	NA	2.86	NA	NA	322	NA	NA	NA	NA	81.2	49.12	7.73	73.3	146	38.4	3.61	61.86	96.51
Pt	NA	15.9	NA	NA	3594	NA	NA	NA	NA	1955	617.74	71.7	1108	2125	470	46.34	534.64	1309.31
Pd	NA	10.33	NA	NA	2675	NA	NA	NA	NA	2993	1548.93	241	3141	5178	1695	113.25	840.29	3482.22
Au	NA	2.71	NA	NA	9.69	NA	NA	NA	NA	224	103.58	16.6	150	307	123	11.55	32.77	162.53

Correlation	Pt	Pd	Rh	Au	Cu	Ni	S
Pt	1	0.85	0.71	0.58	0.52	0.56	0.38
Pd	0.85	1	0.72	0.62	0.62	0.66	0.47
Rh	0.71	0.72	1	0.19	0.13	0.34	0.1
Au	0.58	0.62	0.19	1	0.74	0.45	0.45
Cu	0.52	0.62	0.13	0.74	1	0.66	0.74
Ni	0.56	0.66	0.34	0.45	0.66	1	0.62
S	0.38	0.47	0.1	0.45	0.74	0.62	1

Table 2: Correlation coefficients between the various metals and PGE using the PTM assay database for the project area (9573 samples except for Rh with 2717 samples).